

**Roles of the untranslated region of bromovirus  
genomic RNA in viral multiplication**

**Taiki Narabayashi**

**2015**

# Contents

<b>General Introduction</b>	<b>1</b>
<b>Chapter I</b>	<b>5</b>
<i>Melandrium yellow fleck bromovirus</i> infects <i>Arabidopsis thaliana</i> and has unique characteristics in genomic RNA sequences among bromoviruses	
<b>Chapter II</b>	<b>29</b>
Base-paired structure in the 5' untranslated region is required for the efficient amplification of negative-strand RNA3 in the bromovirus <i>Melandrium yellow fleck virus</i>	
<b>Chapter III</b>	<b>52</b>
Temporal regulation of viral multiplication via the 5' untranslated region of RNA3 of <i>Melandrium yellow fleck virus</i>	
<b>References</b>	<b>76</b>
<b>Summary</b>	<b>87</b>
<b>Acknowledgements</b>	<b>89</b>
<b>List of Publications</b>	<b>90</b>

# General Introduction

Plant diseases are caused by unfavorable environmental conditions, such as lack or excess of nutrients, moisture, and light, and the presence of toxic chemicals in air or soil. This also includes attack by pathogenic microorganisms, such as viruses, viroids, bacteria, fungi and nematodes (Agrios, 2005). Viruses are one of the smallest types of pathogen, and viral particles contain DNA or RNA genomes as well as structural proteins. Some viral particles are surrounded by a host-derived lipid membrane called an envelope. Viral infection in plants induces various symptoms, such as mosaic, yellowing, dwarf, and necrosis, and causes a lot of crop losses, thus it is important to protect plants from diseases. However, control of plant viruses is not well-established, and we should first elucidate the mechanisms of plant virus infection. Successful infection of plants by viruses depends on the interactions between host and viral components for the replication of the viral genome, the expression of viral proteins, the movement of viruses through the individual plant, and the suppression of host defense responses. To understand these mechanisms, it is necessary to determine the factors, involved in plant diseases, with regards to both plant and viral components.

Viruses can be divided into seven major classes based on their genome replication and encapsidation strategies, which are independent of the host species that include plants, animals, and bacteria (Ahlquist, 2006). Viral genomes consist of single- or double-stranded RNA or DNA, indicating that there is diversity in viral replication strategies. About two-thirds of plant virus species belong to the positive-strand RNA virus group, in which the virion contains a messenger-sense single-stranded RNA genome (Hull, 2009).

The genomic RNAs of all positive-strand RNA viruses have multifunctional roles. They act as mRNAs to translate viral proteins and also as the templates for negative-strand RNA synthesis, which in turn acts as the templates for positive-strand RNA synthesis. Newly-synthesized positive-strand RNAs also serve as the mRNAs and as the templates for RNA synthesis, or are packaged into virions. Thus, it is important to regulate these processes, and several RNA elements that are required for these processes have been identified (Dreher, 1999; Noueirry and Ahlquist, 2003; Liu et al., 2009; Ogram and Flanagan, 2011; Pathak et al., 2011). Negative-strand RNA synthesis is initiated near the 3' terminus, but the RNA elements required for negative-strand RNA synthesis are located in the other regions of viral RNAs such as the 5' untranslated region (UTR), as well as in the 3' UTR. The functions of these RNA elements have been investigated, and they are known to be regulated through interactions between viral RNA elements, or between viral RNA elements and proteins, including viral and host factors (Herold and Andino, 2001; Noueirry and Ahlquist, 2003; Filomatori et al., 2006; Pathak et al., 2011).

Bromoviruses, are a well-studied group of icosahedral plant viruses that belong to the alphavirus-like superfamily. The bromovirus genome consists of positive-stranded tripartite RNAs designated RNA1, RNA2 and RNA3 (Lane, 1981). These genomic RNA molecules have a cap structure at the 5' terminus and a tRNA-like structure at the 3' terminus. The intercistronic region (ICR) of RNA3 contains a poly(A) tract. The type member of the genus *Bromovirus* is *Brome mosaic virus* (BMV), and other five viruses have been reported so far in the genus: *Cowpea chlorotic mottle virus* (CCMV), *Broad bean mottle virus* (BBMV), *Spring beauty latent virus* (SBLV), *Cassia yellow blotch virus* (CYBV), and *Melandrium yellow fleck virus* (MYFV) (Roossinck et al., 2005). Full-length cDNA clones have already been constructed for BMV, CCMV, BBMV,

SBLV, and CYBV, from which infectious *in vitro* transcripts have been generated (Ahlquist et al., 1984b; Allison et al., 1988; Fujisaki et al., 2003; Iwahashi et al., 2005; Pogany et al., 1994). The complete genomic RNA sequences of these viruses have been determined (Ahlquist et al., 1981b; 1984a; Allison et al., 1989; Dziaott and Bujarski 1991; Fujisaki et al., 2003; Iwahashi et al., 2005; Romero et al., 1992). RNAs 1 and 2 of BMV encode the 1a and 2a proteins, respectively, which are both required for genomic RNA replication and subgenomic RNA4 synthesis (Kroner et al., 1989; 1990). RNA3 is a dicistronic RNA that encodes the 3a protein required for bromovirus movement (Mise et al., 1993; Schmitz and Rao, 1996), and the coat protein (CP). The CP is translated from the RNA4, which is transcribed from the negative-strand RNA3 (Miller et al., 1985; Sacher and Ahlquist, 1989).

The *cis*-acting RNA elements that are required for the BMV replication are well documented. In the 3' UTR, the stem loop C (SLC) within the tRNA-like structure promotes for negative-strand synthesis (Chapman and Kao, 1999; Kim et al., 2000). The promoter for positive-strand synthesis is located in the 3' UTR of negative-stranded RNA, which is the 5' UTR of positive-stranded RNA (Sivakumaran et al., 1999). The box B motif is located in the ICR of RNA3 and in the 5' UTRs of RNA1 and RNA2. After this motif is recognized by the 1a protein, the genomic RNA molecules are recruited to the endoplasmic reticulum (ER) membrane invaginations where BMV replication occurs (Sullivan and Ahlquist, 1999; Chen et al., 2001; Schwartz et al., 2002). The box B motif located in the 5' UTRs of RNA1 and RNA2 also have been reported to be involved in translational repression by 1a protein and CP, which are key steps in the negative-strand RNA synthesis (Yi et al., 2007; Yi et al., 2009). RNA elements required for specific packaging have also been identified in the tRNA-like structure and in the 3a-coding region (Choi and Rao, 2003; Damayanti et al., 2003).

Although many RNA elements and their functions have been reported, more information of RNA elements is needed to understand the life cycle of RNA viruses like BMV.

MYFV was isolated from *Melandrium album* (*Silene latifolia* spp. *alba*) in Hungary (Hollings and Horváth, 1981). MYFV virions are icosahedral particles of approximately 25 nm in diameter, and they are stable at neutral pH, like SBLV (Hollings and Horváth, 1981; Valverde, 1985). The host range of MYFV is distinct from that of the other five bromoviruses. However, in contrast to the other five bromoviruses, molecular analysis of MYFV has not been reported.

In Chapter I, I described the construction of full-length cDNA clones of MYFV genomic RNA molecules 1, 2 and 3, from which infectious *in vitro* transcripts can be transcribed, determined their complete nucleotide sequences, and found that they contain several unique characteristics compared with the other bromoviruses, especially the duplicated region in the 5' UTR of RNA3. In Chapter II, I described the identification of the base-paired structure in the 5' UTR of RNA3, which is involved in RNA3 amplification. In Chapter III, I described the effect of another base-paired structure in the 5' UTR of RNA3 on CP accumulation. Functions of the 5' UTR of RNA3 in MYFV multiplication are discussed.

# Chapter I

## ***Melandrium yellow fleck bromovirus* infects *Arabidopsis thaliana* and has genomic RNA sequence characteristics unique among bromoviruses**

### **Introduction**

Recently, it has been reported that *Spring beauty latent virus* (SBLV) and *Cassia yellow blotch virus* (CYBV) infect a model plant, *Arabidopsis thaliana*, more efficiently than *Brome mosaic virus* (BMV) and *Cowpea chlorotic mottle virus* (CCMV) (Fujisaki et al., 2003; 2009; Iwahashi et al., 2005). Furthermore, SBLV induced severe necrotic symptoms in some *A. thaliana* accessions, such as S96 (Fujisaki et al., 2004), and CYBV induced mild chlorotic symptoms in S96 (Iwahashi et al., 2005). In this study, I found that *Melandrium yellow fleck virus* (MYFV) also infects an *A. thaliana* accession Col-0 efficiently, but the susceptibility to MYFV of accession S96 is different from that to SBLV and CYBV. This suggests that the use of MYFV in combination with SBLV and CYBV would be useful for analyzing viral factors determining different infectivities between the two bromoviruses in *A. thaliana*.

In this chapter, to establish the molecular basis for analyzing MYFV and to reveal phylogenetic relationships between MYFV and other bromoviruses, I constructed biologically active cDNA clones from which complete copies of the three MYFV genomic RNAs are transcribed, determined the complete nucleotide sequences of MYFV genomic RNAs, and found several unique characteristics compared with the

other bromoviruses.

This chapter corresponds to a paper published (Narabayashi et al., 2009).

## **Results and Discussion**

### *Host range of MYFV*

Infectivity of MYFV was investigated in several plant species that had been used for laboratory experiments with bromoviruses. Plants were inoculated with virion RNA, and accumulation of viral CPs in inoculated and uninoculated upper leaves was assessed by western blot analysis using anti-BMV antiserum at 14 days post inoculation (dpi). Virion RNAs were used as inocula instead of virions to avoid detecting input CP in the inoculated leaves. MYFV systemically infected *Nicotiana benthamiana* like other bromovirus (Table I-1). However, MYFV induced yellowing symptoms in the upper uninoculated leaves, whereas SBLV and CYBV induced green mottling symptoms, and BMV systematically infected *N. benthamiana* without inducing symptoms (Fujisaki et al., 2003; Iwahashi et al., 2005). MYFV systemically infected *Gomphrena globosa* similarly to other bromoviruses (Table I-1), and necrotic spots were observed in the upper uninoculated leaves (data not shown). Although MYFV infected and induced symptoms in the inoculated leaves of *Chenopodium quinoa*, it did not infect barley or cowpea (Table I-1). These data indicate that MYFV is similar to SBLV in host range.

The model plant *A. thaliana* accession Col-0 was inoculated with virion RNAs of MYFV at three to four weeks after sowing. No symptom was observed in the inoculated leaves, while in the upper uninoculated leaves, no or mild yellow spots were observed at

14 dpi. The accumulation of viral CPs in the inoculated rosette leaves and uninoculated upper cauline leaves was assessed by hammer blot analysis. MYFV CP accumulated to high levels in both the inoculated and uninoculated leaves (Table I-1). Similar results were observed for SBLV and CYBV (Fujisaki et al., 2003; Iwahashi et al., 2005). In SBLV and CYBV cases, 63 and 52 *Arabidopsis* accessions, respectively, were inoculated, and most of accessions showed only mild or no symptoms. Sixty-nine in total of the overlapped and some additional accessions were inoculated with MYFV and all showed only mild or no symptoms (Table I-2). Upon infection with SBLV, it was reported that accessions Fr-2, S96, Ei-2 and Abd-0 showed severe growth inhibition (Table I-2; Fujisaki et al., 2004). Similar to this, severe stunting was observed upon CYBV infection in accessions Ei-2 and Abd-0, whereas, in Fr-2 and S96, CYBV infection induced mild chlorotic symptoms and only slightly inhibited growth of the infected plants (Table I-2; Iwahashi et al., 2005). However, in the four accessions, MYFV infection induced no or mild symptoms similar to other accessions (Table I-2). Such differences in responses of *A. thaliana* accessions to MYFV, SBLV and CYBV suggest that MYFV, rather than CYBV, would be more useful for analyzing plant–virus interactions in those particular accessions of *A. thaliana*, when used in combination with SBLV (Iwahashi, F. and Mise, K., unpublished results).

#### *Construction of full-length cDNA clones of MYFV*

To analyze molecular interactions between bromoviruses and *A. thaliana* using MYFV and SBLV, I created a set of infectious cDNA clones of the MYFV genome using the RT-PCR-based method that was developed for SBLV and CYBV (Fujisaki et al., 2003; Iwahashi et al., 2005). Full-length cDNAs of MYFV RNAs were synthesized using

primers designed for both terminal sequences of MYFV RNAs. Transcripts from the cDNA clones were predicted to have one additional G residue at the 5' terminus to enhance the efficiency of transcription. Some extra nonviral residues (GAAUU) or (CGCG) at the 3' terminus of the viral genomic sequences were generated from the *EcoRI* (RNA1) or *MluI* (RNAs 2 and 3) recognition sequence, respectively (Fig. I-1).

Since RT-PCR may have made some misincorporation of nucleotides into full-length cDNAs, leading to missense or nonsense substitution and loss of biological activity, I selected a set of clones for RNAs 1, 2 and 3 from the capped transcripts from the clones of full-length cDNAs of MYFV. These were involved in the production of MYFV-specific symptoms in *N. benthamiana*. So far, to select the RNA3 clone of bromoviruses, the length of the poly(A) tract in the intercistronic region (ICR) of RNA3 has been determined, because the lengths are heterogeneous in each population of bromoviruses (Fujisaki et al., 2003; Iwahashi et al., 2005; Romero et al., 1992). Unexpectedly, however, MYFV did not have the poly(A) tract in the ICR of RNA3. Most cDNA clones of RNA3 had duplication in the 5'UTR and each contained polypyrimidine tract with heterologous length. Thus, instead of the poly(A) tract, I further determined the length of the polypyrimidine tracts in the 5' UTR of the RNA3 sequence (Figs. I-2, 3). The polypyrimidine tracts consist of the consensus sequence 'CU5CUn(C/U)C'. The first poly(U) sequences were constantly 5 residues long, while the second poly(U) sequences varied not only between upstream and downstream tracts within a clone but also between different clones and were 4-11 residues long, with an average of 8.6 residues (Fig. I-3). I chose one infectious RNA3 cDNA clone (#11) which was closest to the average length in the virus population. These representative cDNA clones of MYFV RNAs 1, 2 and 3 were designated pMY1TP1, pMY2TP2 and pMY3TP3, respectively. This set of plasmids and all *in vitro* or *in vivo* products arising

from them are referred to as belonging to the KU1 strain of MYFV. The infectivity of a mixture of the capped transcripts from pMY1TP1, pMY2TP2 and pMY3TP3 and the symptoms induced were identical to those produced by MYFV virion RNAs in the experimental plant species listed in Table I-1 (data not shown). This suggests that the KU1 strain of MYFV well reflects the characteristics of wild-type MYFV.

#### *Genome structure of MYFV*

The complete nucleotide sequences of MYFV RNAs 1, 2 and 3 were determined by sequencing the full-length cDNA inserts of pMY1TP1, pMY2TP2 and pMY3TP3, respectively. The lengths of MYFV RNAs 1, 2 and 3 were 3,249, 2,862 and 2,424 nucleotides, respectively. Four potential ORFs were identified in the genomic RNA sequences of MYFV, as well as in those of the other bromoviruses. In MYFV RNA1, one large ORF occurs, which encodes a protein of 948 amino acids corresponding to the 1a protein of other bromoviruses and containing a methyltransferase-like domain and a helicase-like domain (Ahola et al., 2000; Dzanott and Bujarski, 1991). MYFV RNA2 potentially encodes a protein of 828 amino acids that corresponds to the 2a protein of other bromoviruses and contains an RNA-dependent RNA polymerase (RdRp)-like domain in the central region. MYFV RNA3 contains two ORFs, and is predicted to encode proteins of 295 and 193 amino acids that correspond to the 3a protein and CP of other bromoviruses, respectively.

To discuss phylogenetic relationships of MYFV with other bromoviruses, I compared deduced amino acid sequences between MYFV and five other bromoviruses. However, phylogenetic relationships between these six bromoviruses were different among the four viral proteins (Fig. I-4). A similar result had been described and

discussed previously (Fujisaki et al., 2003; Iwahashi et al., 2005).

I then compared the noncoding regions among these bromoviruses. The 5' ends of genomic RNAs 1, 2 and 3 of MYFV are capped like those of other bromoviruses, which was confirmed by 5' RACE analysis using TAP treatment prior to reverse transcription as described previously (Iwamoto et al., 2001). The 5'-terminal residues of MYFV genomic RNAs are adenine, similar to *Broad bean mottle virus* (BBMV) (Dzianott and Bujarski, 1991), whereas those of the other four bromoviruses are commonly guanine (Dzianott and Bujarski, 1991; Fujisaki et al., 2003; Iwahashi et al., 2005). Moreover, tRNA-like structures were found in the 3' noncoding region of MYFV RNAs. The structure of MYFV, as well as BBMV, lacked a “D-arm”, unlike other bromoviruses including SBLV (Fig. I-2B) (Ahlquist et al., 1981a; Fujisaki et al., 2003; Iwahashi et al., 2005). The 3'-terminal nucleotide sequence of MYFV genomic RNAs are –CCA, which is identical to those of all other bromoviruses.

The 5' noncoding regions of RNAs 1 and 2 of MYFV are quite similar and contain two motifs highly conserved among those of the other bromoviruses. These correspond to canonical boxes A and B in the eukaryotic RNA polymerase III promoter, which is considered to be an internal control region for the replication of viral genomic RNAs (Pogue et al., 1990; Pogue and Hall, 1992). RNA 3s of CCMV, SBLV and BBMV have a relatively long 5' noncoding sequence and contain a subgenomic promoter-like sequence within the region. However, other than some contribution to viral competitiveness (Pacha and Ahlquist, 1992), no significant biological function has been identified for this insertional segment in RNA3. On the other hand, RNA3s of CYBV and BMV have a relatively short 5' noncoding sequence and do not contain a subgenomic promoter-like sequence within the region (Fig. I-2). MYFV RNA3 has not only a relatively long 5' noncoding sequence, containing a subgenomic promoter-like

sequence (date not shown), but also a duplicated sequence about 200 bases, containing short ORF, around the border of the duplicated regions (Fig. I-3). This short ORF corresponds to the 5' proximal sequence of the 3a gene. In BBMV, 21 5' extra nucleotides were found in Bawden strain (Pogany et al., 1994), however, such a long duplication and short ORF were not known in bromoviruses so far. *Alfalfa mosaic virus* (AMV), which belongs to other genus of the *Bromoviridae* family, has some repeat and duplication sequences in the 5' UTR of RNA3 (Langereis et al., 1986). Furthermore, it was reported that AMV strain N20 had two short ORFs (URF1 and URF2) in the 5' UTR of RNA3 and the 5' sequence of URF1 was almost identical to that of MP ORF (Jayasena and Randels, 2004). However, biological significance of those duplication in the 5' UTR of RNA3 has not yet been shown for those viruses. Thus, both the 5' and 3' UTR of MYFV genomic RNAs are much more similar to those of BBMV than to those of other bromoviruses, whereas the intercistronic region (ICR) of RNA3 is distinct even from that of BBMV as discussed below.

The ICR of RNA3 of known bromoviruses contain a poly(A) tract, which is a hallmark of bromoviruses and known to function as a spacer required for efficient subgenomic RNA synthesis *in vivo* (French and Ahlquist, 1988). The average lengths of the tracts of BMV, CCMV, SBLV, CYBV and BBMV are approximately 20, 40, 40, 40 and 70 residues, respectively (Ahlquist et al. 1981b; Allison et al., 1988; Fujisaki et al., 2003; Iwahashi et al., 2005; Romero et al., 1992) (Fig. I-2). By constant, in MYFV, the poly(A) tract is not present. Smirnyagina et al. (1994) demonstrated that deletion of the poly(A) tract resulted in loss of subgenomic RNA4 synthesis and reduced RNA3 accumulation, while alternative ways of activating the BMV subgenomic promoter were possible without the poly(A) tract. MYFV would have a certain sequence instead of the poly(A) tract to activate the transcription of the sgRNA.

The ICR of BMV contains a box B sequence, which is necessary for efficient RNA3 amplification (Sullivan and Ahlquist, 1999). MYFV as well as SBLV and CYBV also contain this sequence, whereas CCMV and BBMV do not (French and Ahlquist, 1987; Fujisaki et al., 2003; Iwahashi et al., 2005; Pacha et al., 1990). Consequently, overall sequences of genomic RNAs of MYFV are quite unique in the six bromoviruses.

#### *Comparison of two clones of MYFV RNA3*

When I selected the RNA3 cDNA clones, I determined the nucleotide sequences of 20 clones and found two clones that lacked the duplication in the 5' UTR of RNA3 (Fig. I-3). One of these clones (designated pMY3TP4) had a nucleotide sequence identical to that of pMY3TP3, except for the duplication. *In vitro* transcripts from this clone, together with those from the RNA1 and RNA2 cDNA clones of MYFV, induced symptoms in *N. benthamiana* and *C. quinoa* and infected *A. thaliana*, like the transcripts from pMY3TP3 (data not shown).

The cDNA insert in pMY3TP3 contained the duplication and the short ORF encoding the seven N-terminal amino acids of the 3a protein and an extra leucine, whereas that in pMY3TP4 did not (Figs. I-5A and I-6). Hereafter, the *in vitro* transcripts from pMY3TP3 and pMY3TP4 are referred to as 3W and 3S, respectively. 3W and 3S had the same infectivities as those described above. However, in *N. benthamiana*, the majority (18 of 20) of MYFV RNA3 clones had the duplication, like 3W (Fig. I-3). Therefore, this duplicated sequence may affect the infectivity of MYFV in *N. benthamiana*.

To verify this hypothesis, I first performed a protoplast assay. In these experiments, all the inoculation experiments were performed with either or both of these RNA3

clones, together with transcripts from RNA1 and RNA2 cDNA clones. Northern blot analysis showed that the accumulation of the viral RNAs was indistinguishable in the protoplasts inoculated with 3W or 3S (Fig. I-5B). Next, I tested the accumulation of viral RNAs in the inoculated and uninoculated leaves of *N. benthamiana* by northern blot analysis. The accumulation was similar between these clones at 14 dpi (Fig. I-5C). Thus, in individual infections, no effect of the duplication was observed. I then inoculated *N. benthamiana* plants with an equimolar mixture of these clones to examine their direct competition during infection. Because the electrophoretic mobilities of 3W and 3S were different (Fig. I-5B), the competition of the RNA3 populations could be examined by northern blot analysis. At 14 dpi, only 3W accumulated in the inoculated leaves of 7 of 16 of the inoculated plants (Fig. I-5C #1). In the other nine plants, 3W accumulated together with 3S, although 3W constituted  $74.2 \pm 8.3\%$  of the total RNA3 (3W plus 3S; Fig. I-5C #2). In contrast, only 3W was detected in the uninoculated upper leaves (Fig. I-5C). This competitiveness in infection has been observed in wild-type CCMV and its deletion mutants (Pacha and Ahlquist, 1992). However, in CCMV, the deletion mutants were less competitive because they lacked elements that enhance infection, whereas in MYFV in this study, competitive success was affected by additional elements: the duplication and the short ORF. Further experiments are in progress to explore these new elements with roles in MYFV infection.

## **Materials and Methods**

### *MYFV and isolation of viral RNA*

*Nicotiana benthamiana* plants were mechanically inoculated with MYFV, and virions were purified at two weeks postinoculation (pi), as described previously (Hollings and Horváth, 1981). Viral RNAs were isolated from purified virions, as described previously (Kroner and Ahlquist, 1992).

#### *Plant materials, growth conditions, and virus inoculation*

*N. benthamiana*, *Gomphrena globosa* L. cv. Buddy Mix, barley (*Hordeum vulgare* L. cv. Hinodehadaka), cowpea (*Vigna unguiculata* cv. California Blackeye), *Chenopodium quinoa* and *Arabidopsis thaliana* accessions were maintained at 25 °C with 16 h illumination per day as described previously (Fujisaki et al., 2003; Pacha and Ahlquist, 1992; Sasaki et al., 2001). *Melandrium album* was grown under the same condition as that for *C. quinoa*. All plants were mechanically inoculated with virions (0.5 µg/µl), virion RNAs (0.1 µg/µl) or a mixture of MYFV transcripts (0.1 µg/µl in total), as described previously (Ahlquist et al., 1984b). The two largest leaves of *N. benthamiana*, *G. globosa* and *C. quinoa*, were inoculated four weeks after sowing, and the primary leaves of barley and cowpea were inoculated one week after sowing. The fully expanded rosette leaves of *A. thaliana* were inoculated three to four weeks after sowing.

#### *Western blot analysis*

Infected leaves were ground in Laemmli's sample buffer (Laemmli, 1970) and subjected to sodium dodecyl sulfate-polyacrylamide gel electrophoresis (SDS-PAGE). A western blot analysis was carried out as described previously (Damayanti et al., 1999). The rabbit anti-BMV antiserum (Iwahashi et al., 2005) was used to detect the CPs of

MYFV.

*Determination of terminal sequences of MYFV RNAs*

cDNA fragments corresponding to the 5' and 3' proximal regions of the 1a and 2a open reading frames (ORFs) of MYFV were amplified by RT-PCR using four sets of degenerate primers as described previously (Fujisaki et al. 2003; Table I-3). The nucleotide sequence of the cDNA fragments were determined and used to determine both the 5' and 3' terminal sequences of MYFV genomic RNAs 1 and 2 by rapid amplification of the cDNA ends (RACE) (Frohman, 1990). Before 5' RACE, virion RNAs were treated with or without tobacco acid pyrophosphatase (TAP) (Nippon gene, Tokyo, Japan) under the conditions recommended by the manufacturer. Because the 3' end sequence of the genomic RNAs of known bromoviruses are highly conserved among RNAs 1, 2, and 3, MYFV RNA3 was reverse transcribed using a primer (Table I-3) designed according to the nucleotide sequences of RNAs 1 and 2 of MYFV. Second strands were then synthesized, and the fragments were cloned as described previously (Gubler and Hoffman, 1983). Both the 5' and 3' terminal sequences of MYFV RNA3 were determined by the 5' and 3' RACE method as well as those of RNAs 1 and 2.

*Construction and in vitro transcription of full-length cDNA clones*

Full-length cDNAs of MYFV RNAs 1, 2 and 3 were amplified using appropriate primers (Table I-3) as described previously (Fujisaki et al., 2003). Fig. I-1 shows the nucleotide sequences around both termini of viral sequences in the cDNA clone plasmids. The primers for MYFV RNA1 contained *NotI* and *EcoRI* sites, while those

for MYFV RNAs 2 and 3 contained *NotI* and *MluI* sites for cloning. *EcoRI* or *MluI* sites were introduced for linearization of the plasmid DNA clones (Fig. I-1). The 5' primers contained the T7 promoter sequence. To enhance the efficiency of *in vitro* transcription, an extra G residue was added to the 5' terminus of the MYFV genomes (Fig. I-1) because the addition of a single extra 5' G residue does not have any detrimental effect on infection with transcripts for the bromovirus, BMV (Janda et al., 1987). pUC118 (Takara, Otsu, Japan) was digested with *HindIII* and *EcoRI* and ligated with a green fluorescent protein (GFP) gene (Chalfie et al., 1994) which has *NotI* site and *MluI* site at both ends, creating pUC118GFP. Amplified cDNA fragments were purified on 1% low-melting-point agarose gels, and the resulting double-stranded cDNA, which contained a full-length copy of MYFV RNA1, was cut with *NotI* and *EcoRI* and ligated into *NotI* and *EcoRI*-cut pUC118GFP (Fig. I-1A). The amplified cDNAs of MYFV RNAs 2 and 3 were cut with *NotI* and *MluI* and ligated into *NotI* and *MluI*-cut pUC118GFP (Fig. I-1B). Three representative full-length cDNA clones for MYFV RNAs 1, 2 and 3 were named pMY1TP1, pMY2TP2, and pMY3TP3, respectively. *In vitro* transcripts from *EcoRI* (RNA1)- or *MluI* (RNA2, 3)-linearized cDNA clones were synthesized using T7 RNA polymerase (Takara) in the presence of m<sup>7</sup>GpppG (New England Biolabs, Beverly, MA, USA), as described previously (Kroner and Ahlquist, 1992).

#### *Sequencing of MYFV genomic cDNA clones and data analysis*

The complete nucleotide sequences of the full-length cDNAs of MYFV RNAs 1, 2 and 3 were determined by primer walking strategy (Table I-4). The full-length cDNAs were sequenced using an automated DNA sequencer (model 310, Applied Biosystems). The

nucleotide and amino acid sequence data were analyzed using DNASIS-Mac v. 3.6 software (Hitachi, Tokyo, Japan) and the CLUSTAL W program (Thompson et al., 1994), respectively. Phylogenetic analyses of the six bromoviruses were performed using the MEGA2 program (Kumar et al., 2000), and phylogenetic trees were constructed with the Neighbor-Joining (NJ) method (Saitou and Nei, 1987).

### *Protoplast experiments*

*N. benthamiana* protoplasts were prepared and inoculated with viral RNA transcripts essentially as described by Navas-Castillo et al. (1997) with modifications. The newest fully expanded leaves were cut with a sharp razor blade at 1 mm intervals, incubated 16 h at 25 °C in the dark in enzyme solution [1% cellulase Onozuka RS (Yakult Honsha, Tokyo, Japan), 0.5% Macerozyme R-10 (Yakult Honsha) in MMC (0.5 M mannitol, 10 mM CaCl<sub>2</sub>, 5 mM MES, pH 5.7)]. Protoplasts were collected through 3 layers of cheesecloth and washed twice in MMC with centrifugation at 45 × g for 3 min. 3.0 × 10<sup>5</sup> protoplasts concentrated in 0.1 ml MMC were mixed with 7.5 µl of inoculum and with 0.2 ml freshly-prepared PEG solution [1 g of polyethylene glycol (PEG) 4000 (Fluka, #81240, Germany), 0.75 ml of DW, 0.625 ml of 0.8 M mannitol, 0.25 ml of 1M Ca(NO<sub>3</sub>)<sub>2</sub>]. Immediately after mixing well, the suspension was diluted with 2 ml MMC, and kept on ice for 15 min before being centrifugated at 45 × g for 3 min. Protoplasts were washed once with 4 ml of MMC and incubated in 0.5 ml of incubation solution [0.5 M mannitol, 1 × Aoki solution (pH 6.5), 4 mM MES (pH 5.7), 200 µg/ml chloramphenicol] at 25 °C for 20 h.

### *Northern blot analysis*

Northern blot analysis of total RNA was performed as described (Damayanti et al., 1999). To construct pMY1MX501, pMY2MX502, and pMY3MH503 for detection of MYFV RNAs 1, 2, and 3, respectively, the 0.2-kb *XhoI/ EcoRI* fragment of pMY1TP1 and pMY2TP2, and 0.2-kb *EcoRV/ EcoRI* fragments of pMY3TP3 were cloned into pBluescript II (KS-) (Stratagene, La Jolla, CA). (+)-strand RNAs of MYFV RNAs were detected using a mixture of DIG-18abeled T7 transcripts from *EcoRI*-linearized pMY1MX501 and pMY2MX502 and *MluI*-linearized pMY3MH503.

**Table I-1** Infectivity of bromovirus virion RNAs

Plant	MYFV		BMV		SBLV		CYBV	
	I	U	I	U	I	U	I	U
<i>Nicotiana benthamiana</i>	+	+	+	+	+	+	+	+
<i>Gomphrena globosa</i>	+	+	+	+	+	+	+	+
<i>Barley</i>	–	–	+	+	–	–	–	–
<i>Cowpea</i>	–	–	–	–	–	–	+	–
<i>Chenopodium quinoa</i>	+	–	+	+	+	–	+	–
<i>Arabidopsis thaliana</i> (Col-0)	+	+	–	–	+	+	+	+

I, inoculated leaves; U, uninoculated upper leaves; +, CP detected; –, CP not detected. Western blot analysis using anti-BMV antiserum was performed at 14 dpi on plant leaves uninoculated and inoculated with virion RNAs (0.1 µg/µl), as described previously (Ahlquist et al., 1984b).

**Table I-2** *A. thaliana* accessions grouped according to the symptom phenotypes induced by infection with MYFV, CYBV, or SBLV

Accessions	Symptoms		
	MYFV	CYBV	SBLV
<i>Abd-0, Ei-2</i>	None or mild	Severe stunting	Severe stunting
<i>Fr-2, S96</i>	None or mild	Mild chlorosis	Severe necrosis
Aa-0 <sup>a</sup> , Ag-0, Ak-1, An-1, Ang-0, Bay-0, Bch-0, Be-0, Berkeley, Bla-2, Bs-1, Bsch-0, C24, Chi-0, Co, Col-0, Col-3 <sup>c</sup> , Da-0, Db-0, Di-1 <sup>a</sup> , Di-G, Dra-0, Ema-0 <sup>a</sup> , En-D, ENF, EN-T <sup>a</sup> , EST, Fe-1, Ga-0 <sup>b</sup> , Gd-1, Gr-3 <sup>a</sup> , H55 <sup>a</sup> , Hl-0 <sup>b</sup> , Hodja-Obi-Garm <sup>b</sup> , Je54 <sup>a</sup> , Jm-1 <sup>b</sup> , Kondara <sup>b</sup> , Kl-0, Landsberg, LIN, Litva, Mh-0, Nd-1, Nw-0 <sup>b</sup> , Ob-0, Old-1, Oy-1, Petagolf <sup>b</sup> , Pi-0, Pla-0, Po-0 <sup>c</sup> , RLD-1, Rubezhnae-1 <sup>b</sup> , Santaclara <sup>a</sup> , Sg-1, Sn <sup>b</sup> , Sorbo, Ta-0 <sup>a</sup> , Tol-0, Tsu-1, Tu-0, Wc-1, Wil-1 <sup>b</sup> , Wt-1 <sup>b</sup> , Wu-0	None or mild	None or mild	None or mild

The results for CYBV and SBLV were reported by Iwahashi et al. (2005) and Fujisaki et al. (2004), respectively. Hammer blot analysis (Fujisaki et al., 2009) showed that all the listed accessions were systemically infected with MYFV.

<sup>a</sup> Not reported for either CYBV or SBLV.

<sup>b</sup> Not reported for CYBV.

<sup>c</sup> Not reported for SBLV.

**Table I-3.** Nucleotide sequence of primers for construction of MYFV infectious cDNA clones

	Primer	Nucleotide sequence	
<b>A</b>	5' side	SB1.1	5'-CATNGCNCRTCRAACAT-3'
		SB1.2	5'-GCNGARCAYTAYGAYTG-3'
		SB2.1	5'-TCRTCRAARTANGCRTG-3'
		SB2.2	5'-GTNCCNTCNTTYCARTGG-3'
	3' side	SB1.9	5'-TTYGGNGAYACNGARCA-3'
		SB1.10	5'-TTRAANARRTCRCAYTT-3'
		SB2.7	5'-TGYGAYMGNATGAARTT-3'
		SB2.8	5'-CCARTYRTGRAACCANTC-3'
<b>B</b>	ANCH	5'-GGCCACGCGTCGACTAGTACTTTTTTTTTTTTTTTTT-3'	
	AUAP	5'-PGCCACGCGTCGACTAGTAC-3'	
	5' RACE	MY1.2	5'-CTTCAAGTGGAAACTGGCCTAG-3'
		MY1.3	5'-AGAACC GCCGAAATCAATAACAG-3'
		MY2.2	5'-AATGAATAATTGTCTAAACGCGAAG-3'
		MY2.3	5'-GTTACTAGGCTCTCCGTTGTTC-3'
		MY3.2	5'-CCGTAACAGTAGAAGAACGACC-3'
		MY3.3	5'-TGGCCTTCTCGGAGAAAATCTC-3'
	3' RACE	MY1.1	5'-AAGCGCAGGGCATTGGGTTG-3'
		MY2.1	5'-TAGACGAAACCGCTTCGTCTTC-3'
MY3.1		5'-GTGCACCTGGAAGTTGAACAC-3'	
<b>C</b>	M4	5'-GTTTTCCCAGTCACGAC-3'	
	RV	5'-CAGGAAACAGCTATGAC-3'	
<b>D</b>	MYFV5'-1,2	5'-ATAAATTGAAGAGAGAGAGGTTCAATTC-3'	
	MYFV5'-3	5'-ATAAAAATAAAATAAAATTCTTTCTAATTGCTTGAC-3'	
	MYFV3'	5'-TGGTCTCCTTTATGACCACC-3'	
	MYFV3'S	5'-TGGTCTCCTTTATGACCAC-3'	
	NotT7-MYFV5'-1,2	5'-ATAAGAATGCGGCCGCTAATACGACTCACTATAG- ATAAATTGAAGAGAGAGAGGTTCAATTC-3'	
	NotT7-MYFV5'-3	5'-ATAAGAATGCGGCCGCTAATACGACTCACTATAG- ATAAAAATAAAATAAAATTCTTTCT-3'	
	NotEco-MYFV3'S-1	5'-ATAAGAATGCGGCCGCAATTC- TGGTCTCCTTTATGACCAC-3'	
	NotMlu-MYFV3'S-2,3	5'-ATAAGAATGCGGCCGCACGCG- TGGTCTCCTTTATGACCAC-3'	
	HindNotGFPr	5'-ATCCCAAGCTTGCGGCCGCTATTGTATAGTTCATCC-3'	
	EcoMluGFPf	5'-CCGGAATTCGACGCGTATGAGTAAAGGAGAAGAAC-3'	

Primers for (A) the synthesis of terminal cDNA clones of MYFV RNA, (B) 5' or 3' RACE, (C) sequencing of partial cDNA clones and (D) MYFV full length cDNA synthesis.

**Table I-4.** Nucleotide sequence of primers for sequencing of MYFV infectious cDNA clones

Primer		Nucleotide sequence			
RNA1	Forward	MY1.11F	5'-GATCTAAGCGCATTACAG-3'		
		MY1.12F	5'-AGTCCAAGCTGATTGGG-3'		
		MY1.13F	5'-CGTAAAATGTCCTCCAG-3'		
		MY1.14F	5'-CAACCATTCAAGAGCAG-3'		
		MY1.16F	5'-GATCAGTGAGTTCACAG-3'		
		MY1.17F	5'-CACATTCCAGTTTGAGAG-3'		
		MY1.18F	5'-CGAAAATGTGGGAATCG-3'		
		MY1.19F	5'-GATGCTTGCCTAAGTTG-3'		
		Reverse	MY1.11R	5'-CTGTAATGCGCTTAGATC-3'	
	MY1.12R		5'-TAGCCCAATCAGCTTGG-3'		
	MY1.13R		5'-CTGGAGGACATTTTACG-3'		
	MY1.14R		5'-CTGCTCTTGAAATGGTTG-3'		
	MY1.16R		5'-CTGTGAACTCACTGATC-3'		
	MY1.17R		5'-CTCTCAAACCTGGAATGTG-3'		
	MY1.18R		5'-CGATTCCCACATTTTCG-3'		
	MY1.19R		5'-CAACTTACGCAAGCATC-3'		
	RNA2		Forward	MY2.11F	5'-CGTTGCTGATGGAAGTC-3'
				MY2.12F	5'-AGAAATCGCAGTCAGCG-3'
		MY2.13F		5'-CTGACTTTAATAAGCTGAAG-3'	
MY2.14F		5'-CCTGTTCGTCAGTAC-3'			
MY2.16F		5'-CGCTACAATCACATTCC-3'			
MY2.17F		5'-GCCATGATGGCATATAC-3'			
MY2.18F		5'-TAAGCCCGGTCTTGAAC-3'			
MY2.19F		5'-CGCTTCGTCTCTTTTTC-3'			
Reverse		MY2.11R		5'-GAGTTCCATCAGCAACG-3'	
		MY2.12R	5'-TCGCTGACTGCGATTTC-3'		
		MY2.13R	5'-CTTCAGCTTATTAAGTCAG-3'		
		MY2.14R	5'-GTATCAGTGACGACAGG-3'		
		MY2.16R	5'-GGAATGTGATTGTAGCG-3'		
		MY2.17F	5'-GTATATGCCATCATGGC-3'		
		MY2.18R	5'-TCAAGACCGGGCTTAAG-3'		
		MY2.19R	5'-AAAAGAAGACGAAGCGG-3'		
		RNA3	Forward	MY3.12F	5'-GGTCGTTCTTCTACTGTTACGG-3'
				MY3.13F	5'-TAATCAAGAGTGCACCG-3'
MY3.14F				5'-CTGTAGAAGAATTAGACG-3'	
MY3.17F	5'-GGTTCAATTCCCCTATGTT-3'				
MY3.18F	5'-CATACCCTTGCCTTCAG-3'				
MY3.19F	5'-CTGCCAGTCATAACTGG-3'				
Reverse	MY3.13R-2		5'-GGTGCCTCTTGATTATC-3'		
	MY3.14R		5'-CGTCTAATCTTCTACAG-3'		
	MY3.17R		5'-GAACATAGGGAATTGAACC-3'		
	MY3.18R		5'-CTGAAGGCAAGGGTATG-3'		
	MY3.19R		5'-CCAGTTATGACTGGCAG-3'		





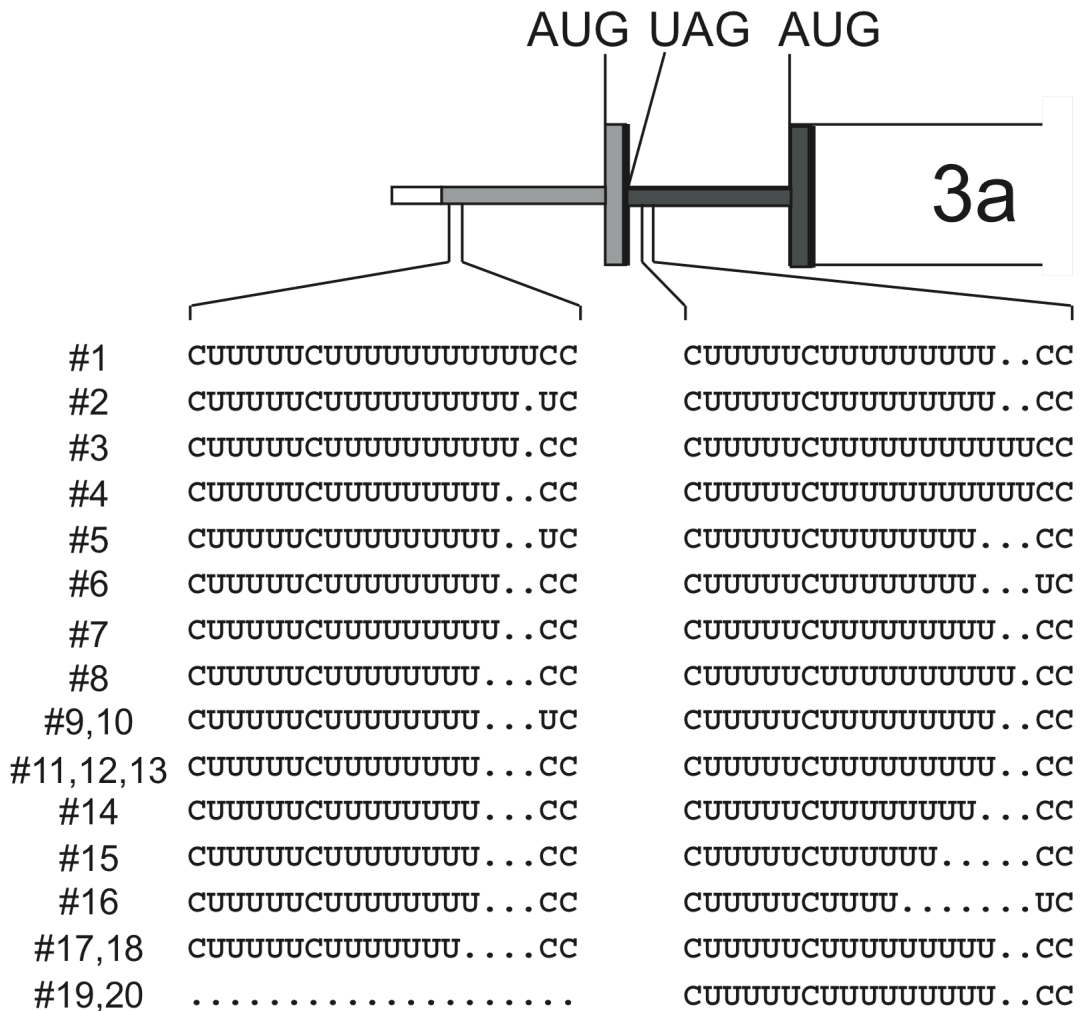


**Fig. I-3. Schematic representation of the 5' UTR of MYFV RNA3 and heterogeneity of two polypyrimidine tracts in the 5' UTR of MYFV RNA3.** The white box indicates the 5' terminal region which is not duplicated. The light gray and dark gray boxes indicate the duplicated region in the 5' UTR of MYFV RNA3. Under the schematic image of the 5' UTR of MYFV RNA3, twenty full-length cDNA clones of MYFV RNA3 and their nucleotide sequences within polypyrimidine tracts are shown. pMY3TP3 is #11 and pMY3TP4 is #19.

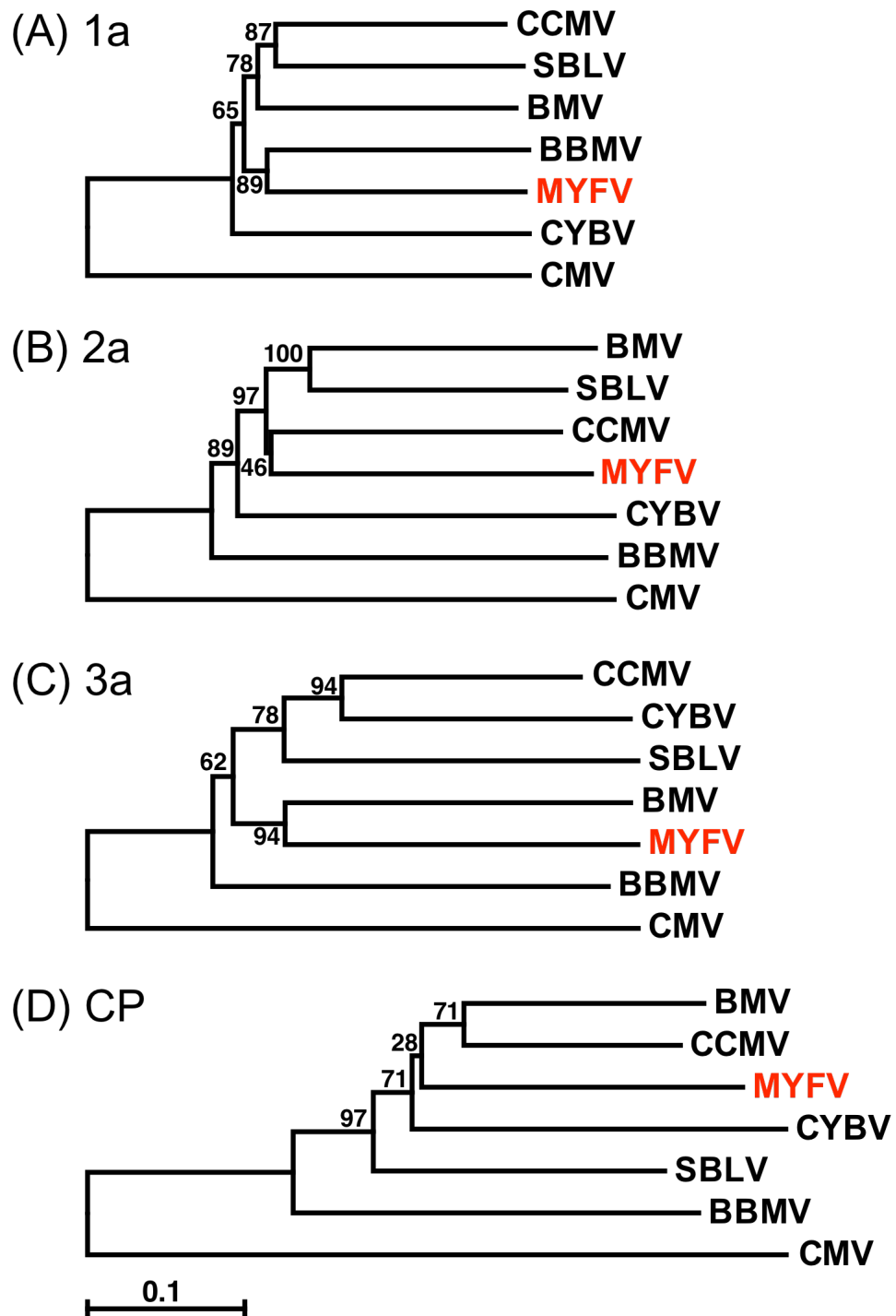


**Fig. I-4. Bootstrap Neighbor-Joining gene trees for bromoviral proteins.** (A) the 1a protein, (B) the 2a protein, (C) the 3a protein and (D) the coat protein (CP) of six bromoviruses, BMV, BBMV, CCMV, CYBV, MYFV and SBLV. An acid sequences of viral proteins from *Cucumber mosaic virus* (CMV) strain serve as the outgroup sequences. Bootstrap values that support clusters indicated above the branch leading to that cluster. The scale represents 0.1 branch length.

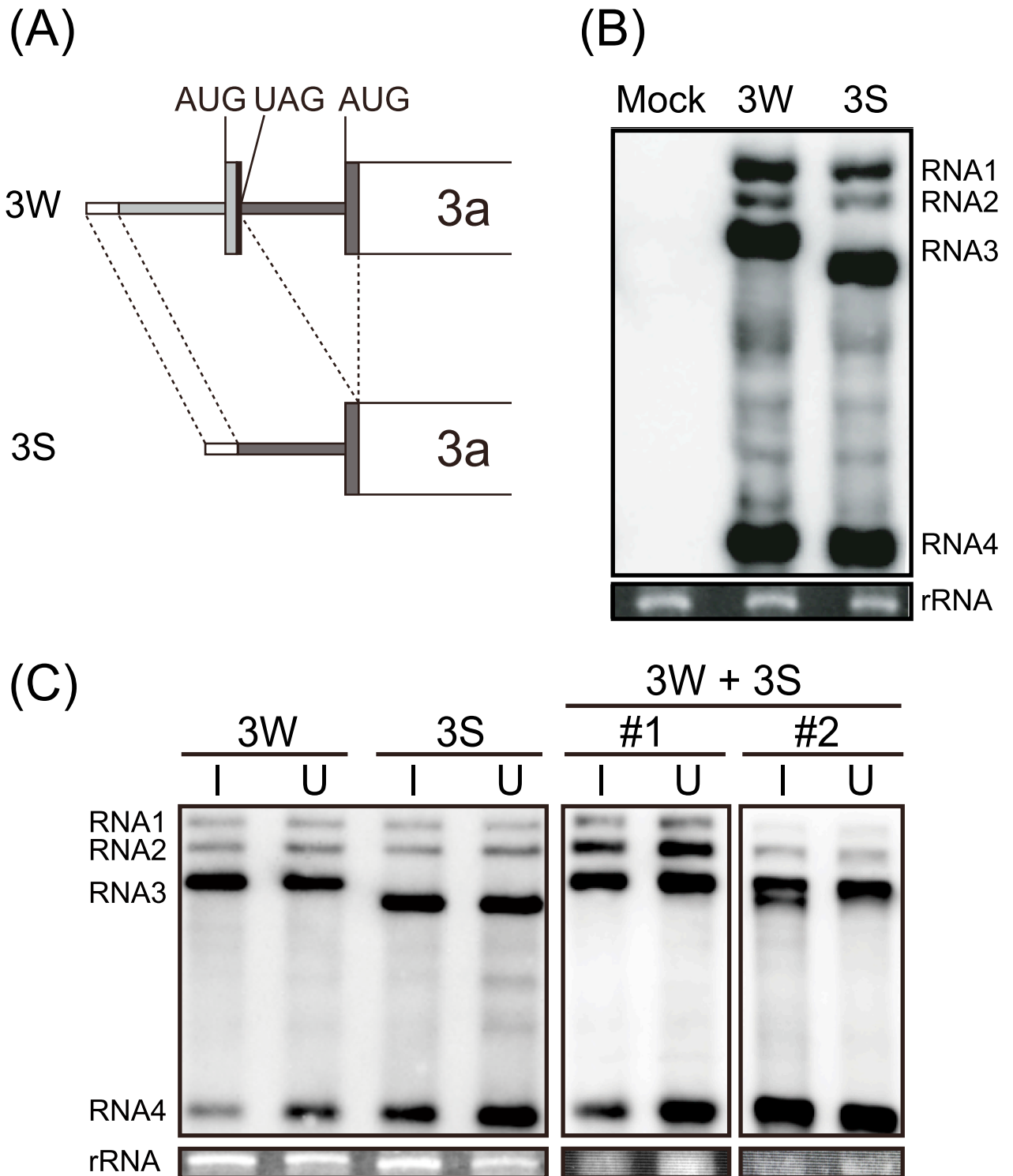


**Fig. I-5 Comparison of two clones of MYFV RNA3.** (A) Schematic image of the 5' UTR of 3W and 3S. Refer to the legend of Fig. 3 for details. (B) *Nicotiana benthamiana* protoplasts were inoculated with MYFV RNA1, RNA2, and RNA3 (3W or 3S). The total RNAs from the protoplasts were separated by electrophoresis on a 1.5% agarose gel, transferred to a nylon membrane, and hybridized with digoxigenin-labelled probes that recognize the 3'-terminal sequences of the MYFV RNAs. Ethidium-bromide-stained rRNA is shown below each lane as a loading control. (C) Northern blot analysis of viral RNA accumulation in the inoculated (I) and uninoculated upper (U) leaves of *N. benthamiana* plants. These plants were inoculated with MYFV RNA1 and RNA2, and either 3W, 3S, or a mixture of equimolar amounts of 3W and 3S. Ethidium-bromide-stained rRNA is shown below each lane as a loading control. As for the mixed inoculation, representative results for two plants (#1 and #2) are shown.

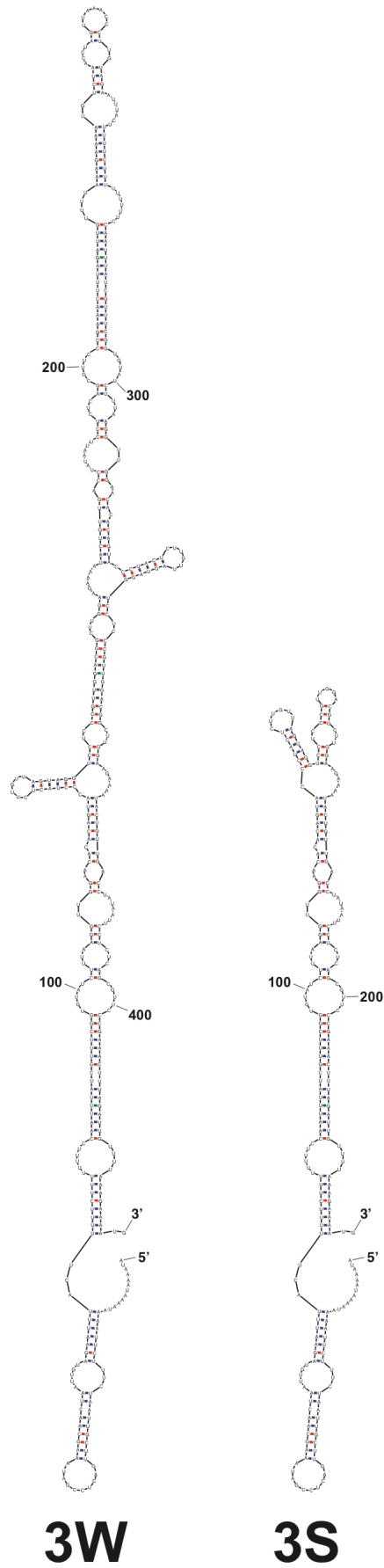


**Fig. I-6. Predicted structures of the 5' UTR of 3W and 3S.** Secondary RNA structures were predicted using M-fold (Zuker, 2003).

## Chapter II

### **Base-paired structure in the 5' untranslated region is required for the efficient amplification of negative-strand RNA3 in the bromovirus *Melandrium yellow fleck virus***

#### **Introduction**

The *cis*-Acting RNA elements required for negative-strand synthesis of genomic RNAs of *Brome mosaic virus* (BMV) are well characterized. In the 3' untranslated region (UTR), the stem loop C (SLC) within the tRNA-like structure acts as the promoter for negative-strand synthesis (Kim et al., 2000). The box B motif in the intercistronic region of RNA3 is recognized by the 1a protein, and then RNA3 is recruited to the endoplasmic reticulum (ER) membrane invaginations where BMV replication occurs (Sullivan and Ahlquist, 1999; Schwartz et al., 2002). The requirement for both the intercistronic region and the 3' UTR of RNA3 for the formation of the replicase complex was demonstrated in yeast system (Quadt et al., 1995), which fully supports BMV replication and transcription as found in plant cells (Janda and Ahlquist, 1993). The 5' UTR of RNA2 also contains the box B motif and has been reported to be involved in translational repression and RNA recruitment, which are key steps during negative-strand RNA synthesis (Chen et al., 2001; Yi et al., 2007). However, although the 5' UTR of RNA3 was also shown to be important for negative-strand RNA3 accumulation (Choi et al., 2004), the detailed roles of the 5' UTR of RNA3 in negative-strand synthesis have remained unclear.

*Melandrium yellow fleck virus* (MYFV) is a member of bromoviruses. MYFV

RNA3 contains a duplicated sequence of about 200 bases with a short ORF around the border of the duplicated regions in the 5' UTR (Fig. I-3). During cDNA cloning procedures, I also found that 10% of the cDNA clones lacked the duplication in the 5' UTR of RNA3. These minor clones had nucleotide sequences identical to those of the other major clones except for the duplication. Co-infection experiments using RNA3 clones with or without the duplicated sequence (3W and 3S, respectively, Fig. II-1A) demonstrated that the duplication contributed to the competitive fitness of the virus in *Nicotiana benthamiana* plants (Fig. I-5). However, the functional role of this duplication in MYFV life cycles has not yet been determined. In this chapter, I used both *N. benthamiana* protoplasts *in vivo* and an evacuated BY-2 protoplast lysate (BYL) *in vitro* (Komoda et al., 2004), and identified a novel RNA element within the duplicated region in the 5' UTR of MYFV RNA3, which is required for the efficient amplification of MYFV RNA3, probably by enhancing negative-strand amplification via specific interactions with its cognate replicase.

This chapter corresponds to a paper published (Narabayashi et al., 2014).

## Results

*The 3W levels were higher than the 3S levels in a competition assay using N. benthamiana protoplasts*

I assumed that the differences in competitive fitness between 3W and 3S in whole *N. benthamiana* plants (Fig. I-5) might reflect the replication efficiency at the single-cell levels. To verify this assumption, I inoculated *N. benthamiana* protoplasts with an

equimolar mixture of 3W and 3S, and RNAs 1 and 2 of MYFV. The Northern blot analysis showed that the levels of RNA3 were similar after individual infection with 3W or 3S, whereas 3W accumulated to 30% higher than 3S following coinfection (Figs. II-1B and 1C). This suggests that there is competition between 3W and 3S, and that the competitive fitness is determined at least partly during the replication step. Given that both of the 5' and 3' terminal regions, as well as intergenic regions, are required for the efficient amplification of BMV RNA3s (French and Ahlquist, 1987), this duplicated region in the internal site of the 5' UTR of MYFV RNA3 might contain previously undefined element(s) that enhance the efficient amplification of bromoviral RNA3.

#### *Regions in the 5' UTR required for efficient amplification of RNA3*

To identify the putative *cis*-acting replication elements in the duplicated region (nt 55-252), I constructed RNA3 derivatives that contained a series of 100-base deletions in the 5' UTR and the 5' proximal sequences of the 3a-ORF (d55-153, d104-202, and d154-252, Fig. II-2A). To exclude the possibility that the effects of the deletion of one element in the duplicated region (light gray region in Fig. II-1A) on RNA3 accumulation may have been masked or attenuated by another element because of the duplication in 3W, I introduced deletions into the 5' UTR of 3S (dark gray region in Fig. II-1A) but not into that of 3W. The resultant RNA3 derivatives, and RNA1 and RNA2, were inoculated into *N. benthamiana* protoplasts, and the accumulation of MYFV RNAs was analyzed by Northern blotting. The d55-153 and d154-252 mutations, but not the d104-202 mutation, reduced the accumulation of RNA3 and RNA4 in protoplasts (Fig. II-2B). These results suggest that the two regions, one from nt 55–103 and the other from nt 203–252, contain nucleotide sequences and/or structures that play

important roles in the accumulation of RNA3 and RNA4.

The d154-252 mutant lacked a partial 5' coding sequence from the 3a gene, so I examined whether this short coding region had any functions in RNA3 accumulation. A d154-226 mutant was constructed with a deletion in the same region as d154-252 apart from the 5' coding region of the 3a gene, which was tested in *N. benthamiana* protoplasts. The accumulation of RNA3 and RNA4 from d154-226 was comparable to that of RNA3 and RNA4 from d154-252 (Fig. II-2B), thereby suggesting that deletions in the 5' UTR of MYFV RNA3 but not the 3a-coding region reduced the accumulation of RNA3 and RNA4 dramatically. Subsequently, I focused on the functions of the 5' UTR of MYFV RNA3 during RNA3 accumulation.

To characterize further the RNA elements involved in RNA3 accumulation, I predicted the secondary RNA structures in the 5' UTR of RNA3 using M-fold version 3.2 (Zuker, 2003), which showed that these two regions (one from nt 55-103 and the other from nt 203-252) formed a long base-paired structure with each other (Fig. II-3A). To delimit the regions that could affect the accumulation of RNA3, I constructed five mutants with deletions covering the two regions in the 5' UTR of RNA3 (d55-64, d65-81, d82-103, d203-217, and d218-229, Fig. II-3B), and I examined their accumulation in *N. benthamiana* protoplasts when they were inoculated together with MYFV RNA1 and RNA2 transcripts. Three deletions (nt 55-64, nt 65-81, and nt 218-229) did not affect the accumulation of RNA3 or RNA4, whereas two deletions (nt 82-103 and nt 203-217) reduced the levels of RNA3 and RNA4 greatly (Fig. II-3C). These two sequences were predicted to form a base-paired structure with each other, which was divided into two stems by an internal loop, thereby suggesting that either or both stems were important for the accumulation of RNA3 and RNA4.

To identify the functional domain and to determine the importance of the

base-paired structure for the accumulation of RNA3, I introduced nucleotide substitutions into either or both sides of the two stems in this region, which disrupted and restored the base-pairing of the stems, respectively (Fig. II-4A). Disruption of the upper stem structure on either side of this region by nucleotide substitutions (r1-1, r1-2) severely decreased the accumulation of RNA3 and RNA4, whereas the restoration of the stem (r1-3) restored the RNA3 and RNA4 levels to that of 3S in *N. benthamiana* protoplasts (Figs. II-4B and 4C). Furthermore, these mutations also affected the accumulation of negative-strand RNA3 in parallel with that of positive-strand RNA3 (Figs. II-4B and 4C). In contrast to the upper stem, the mutations in the lower stem (r2-1, r2-2, r2-3) did not affect the accumulation of positive- or negative-strand RNA3 (Fig. II-4B). Overall, these results suggest that the upper stem structure plays a crucial role in the *in vivo* accumulation of positive- and negative-strand RNA3.

*The base-paired structure is involved in the efficient amplification of negative-strand RNA3*

The mutations in the base-paired structure reduced the *in vivo* accumulation of negative-stranded RNA3 (Fig. II-4), but it was still unclear whether this reduction was caused by decreases in negative- and/or positive-strand RNA3 synthesis. To determine whether this base-paired structure has a role in the amplification of negative-strand RNA3, I performed an *in vitro* translation/replication BYL assay (Komoda et al., 2004). RNA3 derivatives were incubated in BYL that expressed the 1a and 2a proteins of MYFV, and the positive- and negative-strand RNA accumulation levels were examined. Similar to the *in vivo* results (Fig. II-4), the accumulation of negative-strand RNA3 in BYL was again reduced significantly by the disruption mutations (r1-1, r1-2) and recovered by the restoration mutation (r1-3) (Fig. II-5). However, the levels of

positive-strand RNA3 in BYL were not changed significantly by either the disruption (r1-1, r1-2) or restoration (r1-3) of the structure in either the presence or absence of the 1a and 2a proteins of MYFV (Figs. II-5A and II-6, data not shown). Together, these results mainly reflected the stability of the input transcripts rather than the levels of newly synthesized positive-strand RNA3, as discussed below. These *in vitro* results suggest that the reduction in negative-strand accumulation in protoplasts was attributable at least partly to a reduction in the efficient amplification of negative-strand RNA3 but not necessarily to the indirect effect of the inefficient amplification of positive-strand RNA3. The results also suggest that this base-paired region (nt 89-95 and nt 203-209) in the 5' UTR of RNA3 is involved in the efficient amplification of negative-strand RNA3, thereby affecting the accumulation of both negative- and positive-strand RNA3s and subgenomic RNA4 in protoplasts (Fig. II-4B).

#### *Comparison between MYFV and other bromoviruses*

Next, I investigated whether the base-paired structure of the 5' UTR of RNA3 was also seen in other bromoviruses. In the 5' UTRs of bromoviruses, base-paired structures that comprised 7-8 base pairs containing the initiation codon (AUG) of 3a-ORF were predicted using the M-fold program (Fig. II-7A). The base-paired structure of MYFV did not contain the AUG sequence, but the four consecutive base pairs (5'-UCGG-3')/(5'-CCGA-3') were conserved among MYFV, BMV, and CCMV (Fig. II-7). In addition, the results shown in Fig. II-4 demonstrate the importance of the structure rather than the sequence for the efficient amplification of MYFV RNA3. Thus, I hypothesize that these base-paired structures may have functions during the efficient amplification of bromoviral RNA3.

To test whether a similar base-paired structure in RNA3 of another bromovirus, BMV, functions during the amplification of MYFV RNA3, I introduced mutations into the 5' UTR of MYFV RNA3. The d-MB1 mutation deleted most of the base-paired structure, except for three G-C pairs (nt 65-92 and nt 206-229 deletions). The d-MB2 mutation was a four-base insertion into d-MB1, which formed a base-paired structure similar to that in BMV. The d-MB3 mutation replaced of the base-paired region of MYFV with the corresponding region of the BMV sequence (Fig. II-8A). These mutants were tested to determine their accumulation levels in *N. benthamiana* protoplasts, which were inoculated together with MYFV RNA1 and RNA2 transcripts, as described above. Northern blot analysis showed that RNA3 accumulation was eliminated by the d-MB1 mutation, whereas it was restored by the d-MB2 and d-MB3 mutations (Fig. II-8B). These results suggest that the base-paired structure of MYFV RNA3 can be replaced with the corresponding structure of BMV RNA3, thereby confirming the importance of the structure rather than the sequence.

To determine whether the base-paired structure of BMV RNA3 is involved in efficient amplification of the parental genome, two deletion mutations were introduced into the 5' UTR of BMV RNA3 (Bd1: nt 79-91 and Bd2: nt 53-91), which resulted in disruptions of the base-paired structure of BMV (Fig. II-8C). When these mutants were inoculated together with BMV RNA1 and RNA2 into *N. benthamiana* protoplasts, the deletions slightly reduced RNA3 accumulation and increased RNA4 accumulation (Fig. II-8D). BMV RNA3 could be replicated after inoculation with MYFV RNA1 and RNA2 (Fig. II-8D), so I also examined the accumulation of Bd1 and Bd2 in the presence of MYFV RNA1 and RNA2. The deletions eliminated the accumulation of RNA3 and RNA4 (Fig. II-8D). Thus, the base-paired structure of BMV RNA3 was essential for the efficient amplification of RNA3 by MYFV replicase, whereas this

structure was not crucial for RNA3 amplification by BMV replicase. These results suggest that the function of the base-paired structure is correlated with the properties of the MYFV replicase.

## **Discussion**

In this study, I analysed RNA elements in the 5' UTR of bromoviral RNA3 that enhance RNA3 amplification. The function of the RNA element required for the efficient amplification of the negative-strand RNA3 of MYFV was shown to be sequence independent but structure dependent, and it was identified as the base-paired structure in the 5' UTR of MYFV RNA3, analogues of which were also found in other bromoviral RNA3s. My analysis of the effects of structural elements in BMV RNA3 demonstrated that the requirement for base-paired structures for RNA3 amplification differed among distinct bromoviral replicases.

The 5' UTR of positive-strand RNA genomes corresponds to the 3' UTR of the negative-strand, which contains a promoter for positive-strand RNA synthesis. Thus, mutations in the 5' UTR could affect positive-strand RNA synthesis. In BMV, mutations in the 5' UTR of RNA3, which affected the promoter activity of positive-strand RNA3 synthesis, had only modest effects on negative-strand RNA3 accumulation, despite the low accumulation of positive-strand RNA3s (Hema and Kao 2004). Moreover, several mutations that substantially decrease positive-strand RNA3 accumulation increased subgenomic RNA4 accumulation (Hema and Kao, 2004; Grdzlishvili et al., 2005). These viral RNA accumulation patterns were also observed in our deletion analysis of the base-paired structure of BMV RNA3 when it was inoculated with BMV RNAs 1 and 2 (Fig. II-8D). Thus, if the base-paired structure of

the 5' UTR of bromoviral RNA3 functions during positive-strand synthesis but not during negative-strand synthesis, mutations in this structure should change the levels of positive-strand RNA3 relative to that of subgenomic RNA4 but would have only mild effects on negative-strand accumulation. However, disruptions of the base-paired structures of the 5' UTR of RNA3s dramatically reduced the accumulation of negative- and positive-strand RNA3 and subgenomic RNA4 *in vivo* (Figs. II-4, 8B and 8D). Therefore, although I cannot exclude the possibility that the base-paired structures may play an additional role in positive-strand RNA3 synthesis by MYFV replicase, similar to that by BMV replicase, the results of the protoplast assays strongly suggested that the base-paired structure functions mainly during the efficient amplification of negative-strand RNA3.

In the *in vitro* BYL assays, the accumulation of positive-strand RNA3 was indistinguishable among 3S and its derivatives (Fig. II-5), which did not correlate with that of negative-strand RNA3. Capped transcripts are stable in BYL, large portions of input transcripts could be detected even after incubation for several hours (Fig. II-6, Sarawaneeyaruk et al., 2009). Moreover, RNA4 accumulation was never observed (data not shown), suggesting that positive-strand RNA synthesis from negative-strand RNA3 was negligible. Therefore, most, if not all, of the positive-stranded RNA3s detected reflected input transcripts, which indicated that the low accumulation of negative-strand RNA3 *in vitro* was not a major consequence of the indirect effects of low positive-strand RNA3 synthesis. These *in vitro* results support the *in vivo* results obtained with protoplasts, and they also indicate that the base-paired region in the 5' UTR of MYFV RNA3 is involved in the efficient amplification of negative-strand RNA3.

The 5' UTR of BMV RNA3 is not required for the formation of the

RNA-dependent RNA polymerase complex (Quadt et al., 1995) or for replicase binding (Choi et al., 2004). My results also showed that the base-paired structure of BMV RNA3 exerted only modest effects on RNA amplification directed by BMV replicase compared with that directed by MYFV replicase (Fig. II-8D). In *Cowpea chlorotic mottle bromovirus* (CCMV), deletions of the regions containing the base-paired structure that corresponded to that of MYFV (Fig. II-8D) had little effect on RNA3 accumulation, whereas deletions of another region of the 5' UTR suppressed the accumulation of RNA3 and RNA4 (Pacha et al., 1990). Thus, although the 5' UTR of bromovirus RNA3s might have general effects on the amplification of the negative-strand RNA3s of bromoviruses, it is not known whether the base-paired structures of BMV and CCMV RNA3s play roles during RNA3 replication by their own replicases. However, the base-paired structure of BMV was shown to function during the efficient amplification of RNA3 (Fig. II-8), possibly by enhancing the amplification of negative-strand RNA3 in the presence of the heterologous replicase of MYFV. This variable requirement of the base-paired structure by distinct bromoviral replicases (Fig. II-8D) suggests that in contrast to BMV, the base-paired structure in the 5' UTR of RNA3 may be required for replicase assembly in MYFV.

In positive-strand RNA viruses, the transition from the translation to the replication of genomic RNAs is a key step during the RNA replication cycle because template competition occurs between these two processes (Gamarnik and Andino, 1998). The *cis*-acting elements required for negative-strand synthesis have been found in the 5' UTR of their genomic RNAs, and they are thought to regulate the transition through RNA-RNA interactions or RNA-protein interactions (Herold and Andino, 2001; Filomatori et al., 2006). In BMV, the repression of RNA1 and RNA2 translation is regulated by the interaction between the replicase protein 1a and the box B motif in

their 5' UTR, which may be related to replicase assembly (Chen et al., 2001; Yi et al., 2007), whereas the RNA3s of four bromoviruses including BMV and MYFV contain the box B motif in the intercistronic region. In two other bromoviruses, CCMV and *Broad bean mottle virus*, the RNA3s do not even contain the box B motif (Allison et al., 1989; Romero et al., 1992). Thus, although some host factors have been reported to be involved in the translation and recruitment of BMV RNA3 (Diez et al., 2000; Mas et al., 2006), the detailed mechanisms that regulate translational repression and the transition from translation to replication in RNA3 are still unclear. In this study, I identified a novel RNA element of MYFV RNA3, which is required for the efficient amplification of negative-strand in the 5' UTR of RNA3, and I found that the function is MYFV replicase specific. These findings will facilitate the development of a better understanding of the life cycle of bromovirus RNA3.

## **Materials and Methods**

### *Plasmid construction*

The pMY3TP4 (3S) contains the same cDNA insert found in pMY3TP3 (3W), except it lacks the duplicated region (Chapter I). Before creating a series of plasmids that encoded C-terminal hemagglutinin (HA)-tagged 3a protein, I inserted three nucleotides (GGC) that encoded a glycine spacer sequence and an HA-coding nucleotide sequence (TACCCATACGATGTTCCAGATTACGCT) immediately upstream of the stop codon of the 3a gene in pMY3TP4 (3S), thereby generating pMY3TP4-HA.

All of the primers used in this study are shown in Table II-1. The plasmids with mutations in the 5' UTR of MYFV RNA3 were generated by PCR-mediated

site-directed mutagenesis of pMY3TP4-HA, which is a method referred to as “recombinant PCR” (Higuchi, 1990). The two pairs of primers used for primary PCR to amplify two DNA fragments were M4 plus dn\_R and dn\_F plus MY3.13R-2 (n = 55–153, 104–202, 154–226, 154–252, 55–64, 65–81, 82–103, 203–217 and 218–229). The two resultant DNA fragments were recombined by secondary PCR using M4 plus MY3.13R-2. The amplified DNA fragments were purified, digested with *HindIII* and *AccI*, and ligated into *HindIII* and *AccI*-cut pMY3TP4-HA to generate pMY3TP4-HA-dn (n = 55–153, 104–202, 154–226, 154–252, 55–64, 65–81, 82–103, 203–217, and 218–229). The following seven plasmids were constructed in a similar manner using two or three pairs of appropriate primers for primary PCR. pMY3TP4-HA-rx (x = 1–1, 1–2, 2–1, and 2–2) was constructed using two pairs of primers: M4 plus rx\_R and rx\_F plus MY3.13R-2 (x = 1–1, 1–2, 2–1, and 2–2), respectively. pMY3TP4-HA-dMB-1 was constructed using three pairs of primers: M4 plus dMB-1\_4, dMB-1\_1 plus dMB-1\_3, and dMB-1\_2 plus MY3.13R-2. pMY3TP4-HA-dMB-2 and pMY3TP4-HA-dMB-3 were constructed using two pairs of primers: M4 plus dMB-2\_2 and dMB-2\_1 plus MY3.13R-2 or M4 plus dMB3\_R and dMB3\_F plus MY3.13R-2, respectively.

To construct pBYL2MY1a and pBYLMY2a, cDNA fragments containing the 1a and 2a genes were PCR-amplified from pMY1TP1 and pMY2TP2 (Chapter I) using two pairs of primers: pBYL-MY1a\_F plus pBYL-MY1a\_R and pBYL-MY2a\_F plus pBYL-MY2a\_R (Table II-1), respectively. The amplified fragments were digested with *AscI* and ligated into *AscI*-cut pBYL2 (Mine et al., 2010) in the correct orientation.

BMV derivatives were generated by PCR-mediated site-directed mutagenesis of pB3TP8 (Janda et al., 1987) using the primer pairs Bd1\_F plus Bd1\_R and Bd2\_F plus Bd2\_R (Table II-1). The amplified fragments were digested with *ClaI* and *SphI*, and

ligated into *Clal* and *SphI*-cut pB3TP8 to create pB3TP8-Bd1 and pB3TP8-Bd2, respectively.

#### *In vitro transcription and protoplast experiments*

Transcripts of bromoviral RNAs were synthesized using T7 RNA polymerase (Takara, Otsu, Japan) with the cap structure analog (m<sup>7</sup>GpppG; New England Biolabs, Beverly, MA, USA), as described previously (Kroner and Ahlquist, 1992; Chapter I). mRNAs encoding MYFV 1a and 2a proteins were synthesized from *NotI*-linearized pBYLMY1a and pBYLMY2a. All of the transcripts were purified using Sephadex G-50 (GE Healthcare Bio-Sciences Corp., Piscataway, NJ, USA) gel chromatography.

*N. benthamiana* protoplast assays were performed as described in Chapter I. Typically,  $2\text{--}3 \times 10^5$  protoplasts were inoculated with 3.0  $\mu\text{g}$  of transcripts (1  $\mu\text{g}$  each for RNA1, RNA2, and RNA3) and incubated at 25 °C for 20 h.

#### *Northern blot analysis*

Northern blot analysis of the total RNA was performed as described in Chapter I. To construct pMY3ES504 for detecting the negative-strand of MYFV RNA3, the 0.4-kb *SacI/EcoRV* fragments of pMY3TP3 were cloned into pBluescript II (SK-) (Stratagene, La Jolla, CA). The negative-strand MYFV RNA3 was detected using digoxigenin (DIG)-labeled T7 transcripts from *EcoRV*-linearized pMY3ES504. The positive-strand BMV RNAs were detected using DIG-labeled riboprobes, which recognized the 3' terminal region of all BMV RNAs (Kaido et al., 1995).

#### *Evacuolated BY-2 protoplast lysate (BYL) experiments*

The preparation of BYL and the *in vitro* translation/replication reaction were performed as described previously (Komoda et al., 2004; Iwakawa et al., 2007). The mRNAs encoding 1a and 2a proteins, which were transcribed from pBYL2-MY1a and pBYL-MY2a, respectively, were incubated in BYL at 25 °C for 2 h. Aliquots (24 µl) of the reaction mixture were further incubated further with bromovirus RNA3 and its derivatives at 25 °C for 2 h. The total RNAs were then extracted and used for Northern blot analysis.

For RNA stability assay, 0.5 µg of capped transcripts were incubated at 25 °C in 40 µl of BYL reaction mixture. At 0, 0.5, 1 and 2 h after incubation, aliquots (10 µl) were used for RNA extraction, and subjected to Northern blot analysis.

**Table II-1**

List of primers and their nucleotide sequences used for PCR to generate constructs

Primer name	Sequence
M4	GTTTTCCCAGTCACGAC
MY3.13R-2	GGTGCACTCTTGATTATC
d55-153_F	CAACTAATTGGACGGCTTGGAAGAAAATAC
d55-153_R	CCAAGCCGTCCAATTAGTTGCTTTATCGG
d104-202_F	CGGTGTATCTCCGAACTTTAGATTG
d104-202_R	CTAAAGTTTTCGGAGATACACCGAAACG
d154-226_F	GTCCTCCCGTTAAAATGTCTAACCTAGTTAAAC
d154-226_R	TTAGACATTTTAACGGGAGGACCTACTAAC
d154-252_F2	GGTCCCTCCCGTTATGACAGGTCGTTCTTC
d154-252_R2	CGACCTGTCATAACGGGAGGACCTACTAAC
d55-64_F	AAAGCAACTAATTCTTTTTCTTTTTTTTCC
d55-64_R	AAAAGAAAAAGAATTAGTTGCTTTATCGG
d65-81_F	TTGTAGAATTTAAATTTATCGTTTCGGTG
d65-81_R	CGATAAATTTAAATTTCTACAATTAGTTGC
d82-103_F	CTTTTTTTTCCCTTAAGGTTGGAACACACAG
d82-103_R	GTTCCAACCTTAAGGAAAAAAAAGAAAAAG
d203-217_F	CCTCTCAGCGTTCGTTTTAAAGAAAATGTC
d203-217_R	CTTTAAAACGAACGCTGAGAGGAATTATAG
d218-229_F	AACTTTAGATTATGTCTAACCTAGTTAAAC
d218-229_R	CTAGGTTAGACATAATCTAAAGTTTCGGG
r1-1_F	GCGTTCGGCTTTGTTTAGATTGTTTTAAAG
r1-1_R	AACAAAGCCGAACGCTGAGAGGAATTATAG
r1-2_F	ATTTATCCAAAGCCTGTATCTTTAAGGTTG
r1-2_R	TACAGGCTTTGGATAAATTGGAAAAAAAAG
r2-1_F	CCGAAACTTATTTAAGTTTTAAAGAAAATG
r2-1_R	CTTTAAAACCTTAAATAAGTTTCGGGAACGC
r2-2_F	TCCTTAGATTTCGTTTCGGTGTATCTTTAAG
r2-2_R	GAAACGAATCTAAGGAAAAAAAAGAAAAAG
dMB-1_1	ATTGTAGAATTTACGGTGTATCTTTAAGG
dMB-1_2	TTAAAGATACACCGTAAATTCTACAATTAG
dMB-1_3	CAGCGTTCCCGATGTCTAACCTAGTTAAAC
dMB-1_4	TTAACTAGGTTAGACATCGGGAACGCTGAG
dMB-2_1	TGTAGAATTTAACATCGGTGTATCTTTAAG
dMB-2_2	TACACCGATGTTAAATTCTACAATTAGTTG
dMB3_F	AGTAGTGATACTGTTTTGTTCCCGATGTCTAACCTAGTTAAAC
dMB3_R	CAAAAACAGTATCACTACTGAAAAAACCGATGTTAAATTCTAC
pBYL-MY1a_F	ATAAGAATGGCGCGCCATGGATCTATTAATTTAATTG
pBYL-MY1a_R	ATAAGAATGGCGCGCCTCAACTTACGCAAGCATC
pBYL-MY2a_F	ATAAGAATGGCGCGCCATGGCTTTCGAAATTGAATATG
pBYL-MY2a_R	ATAAGAATGGCGCGCCTTACTTAGAAAAAGAAGAC
Bd1_F	TAGTGATACTATGTCTAACATAGTTTCTCC
Bd1_R	TTAGACATAGTATCACTACTGAAAAAACCG
Bd2_F	CTATTTTACCAATGTCTAACATAGTTTCTC
Bd2_R	GTTAGACATTGGTAAAATAGAATGTTTCGCC

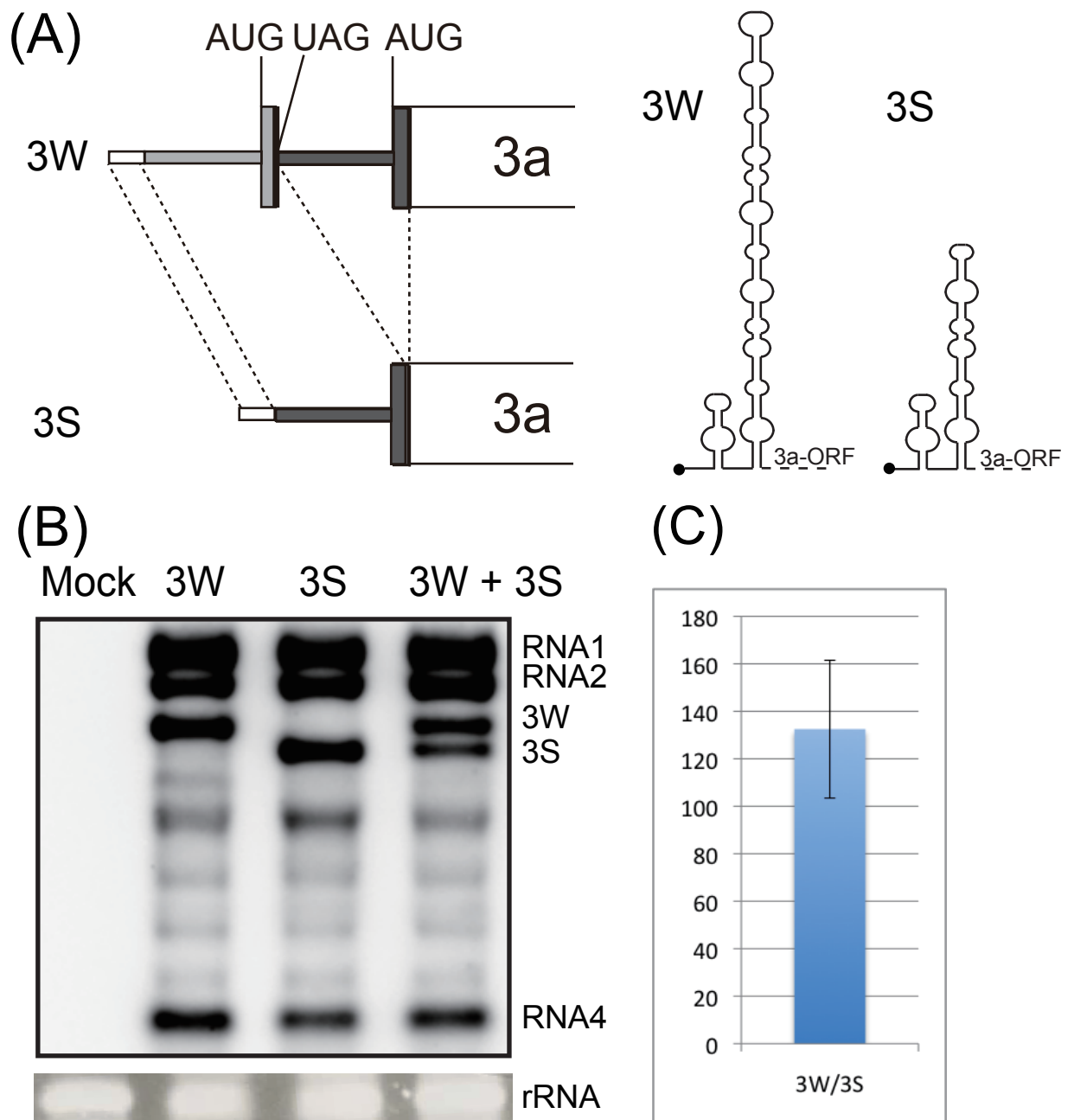


**Fig. II-1. Competition between 3W and 3S in *N. benthamiana* protoplasts.** (A) Schematic representation of the 5' UTR of 3W and 3S. The open bar indicates the 5' terminal region that is not duplicated. The light gray region represents duplicate region of the dark gray region in the 5' UTR of MYFV RNA3. Schematic representation of the predicted structures is also shown. Refer to Fig. I-6 for the predicted structure based on nucleotide sequences. (B) Northern blot analysis of viral RNA accumulation in *N. benthamiana* protoplasts inoculated with a mixture of equimolar amounts of 3W and 3S together with MYFV RNA1 and RNA2. Ethidium bromide-stained rRNA is shown as a loading control. (C) The histogram represents accumulation ratios of 3W compared to 3S at competition. The levels were measured using the ImageJ program and the mean value and the standard deviation were calculated from six independent experiments.

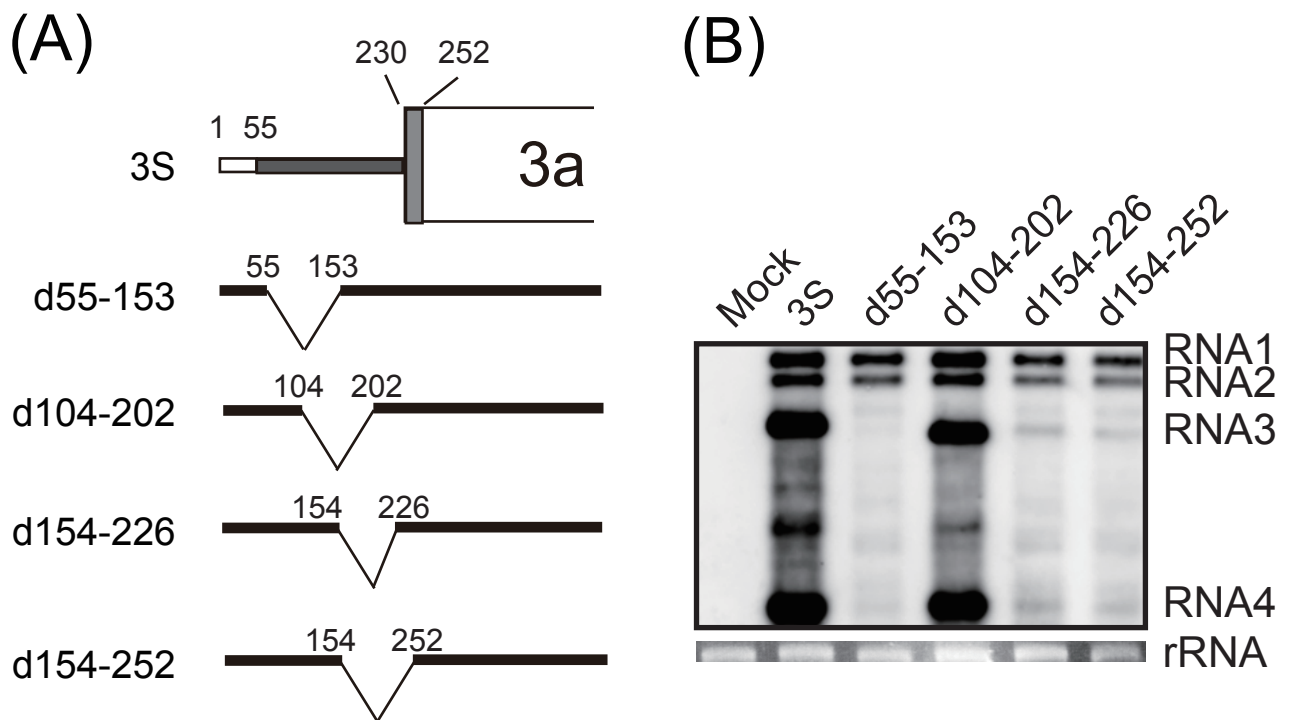


**Fig. II-2. Deletion analysis of the 5' UTR of MYFV RNA3.** (A) Schematic representation of deleted regions in the 5' UTR of 3S. Nucleotide deletions are indicated by a bent line with the nucleotide numbers indicated at their 5' and the 3' ends. (B) Northern blot analysis of viral RNA accumulation in *N. benthamiana* protoplasts inoculated with 3S or its variants together with MYFV RNA1 and RNA2.

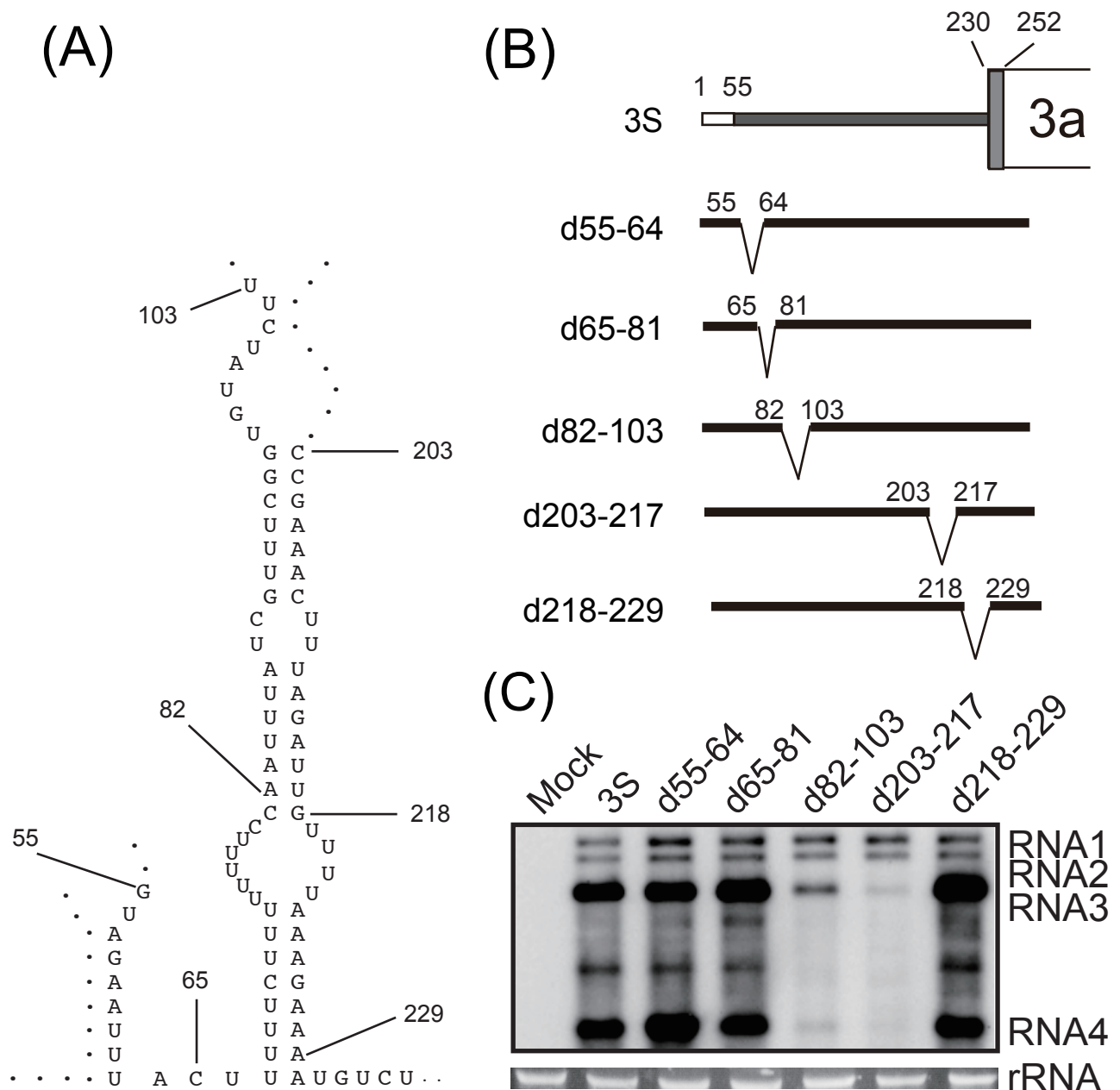


**Fig. II-3. Structure-based deletion analysis of the 5' UTR of MYFV RNA3.** (A) Schematic representation of the predicted secondary structure of the regions including the cis-element involved in 3S amplification. (B) Schematic representation of deleted regions in the 5' UTR of 3S. Nucleotide deletions are indicated by a bent line with the nucleotide numbers indicated at their 5' and the 3' ends. (C) Northern blot analysis of viral RNA accumulation in *N. benthamiana* protoplasts inoculated with 3S or its variants together with MYFV RNA1 and RNA2.



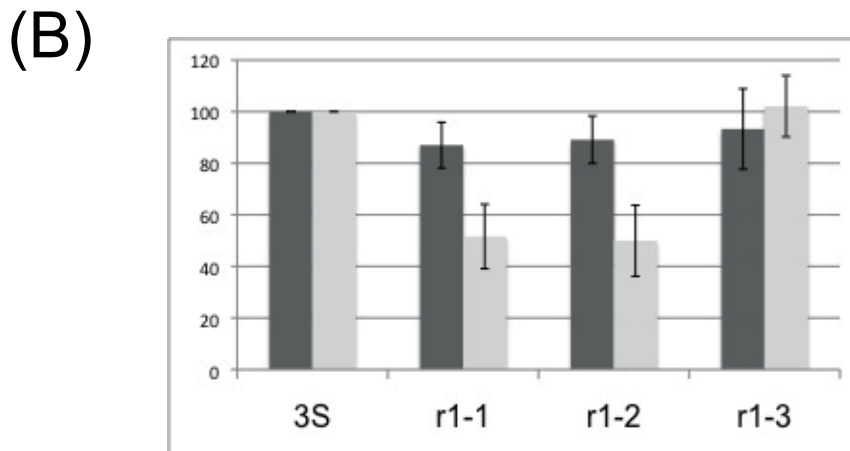
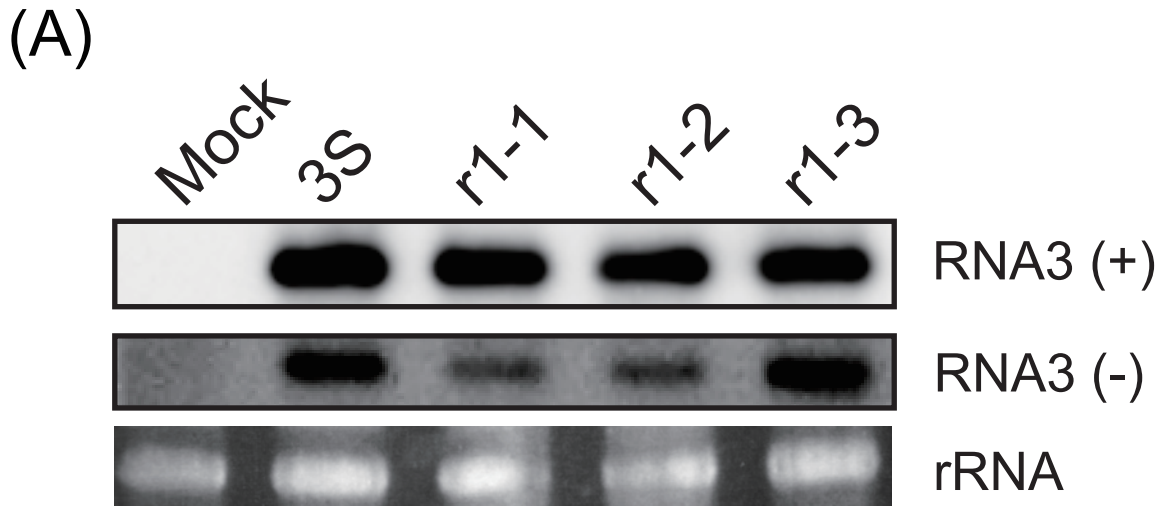


**Fig. II-5. *In vitro* RNA replication assay for the upper stem mutants of MYFV RNA3.** (A) Accumulation of positive- and negative- strand RNA3 in BYL incubated for 2 h with mRNA expressing MYFV 1a and 2a proteins and then for 2 h with 3S or its variants. Total RNA was extracted and subjected to northern blot analysis. A representative result is shown. (B) The histogram compares the levels of positive- (dark gray bars) or negative- (light gray bars) strand of the tested RNA3 derivatives with that of the positive- or negative strand of 3S, respectively. The levels were measured using the ImageJ program and the mean value and the standard deviation were calculated from three independent experiments.

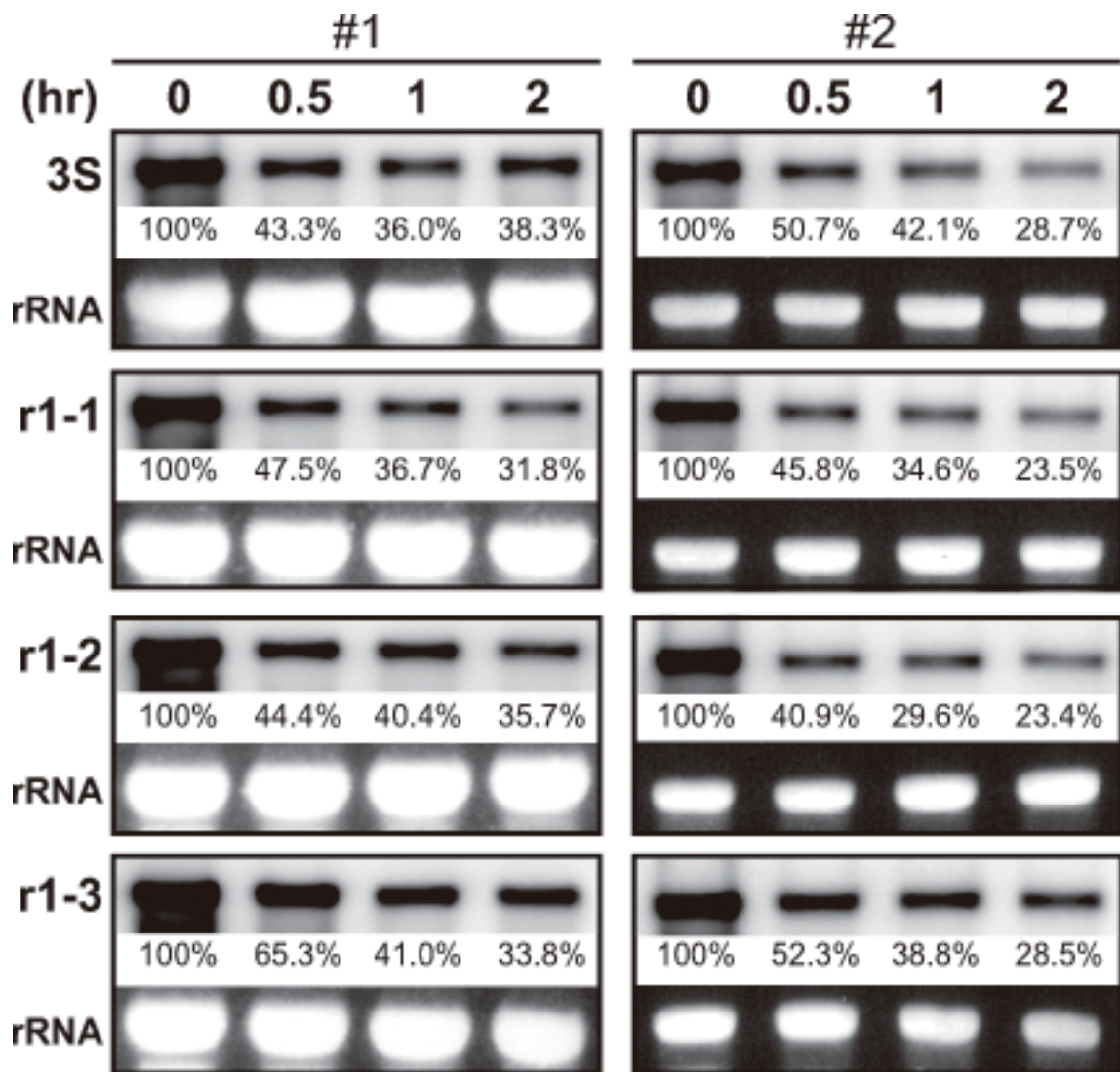


**Fig. II-6. Temporal changes in the accumulation patterns of 3S and its derivatives in two independent experiments (#1 and #2).** RNAs were incubated in a cell-free extract of evacuated BY-2 protoplasts (BYL). Total RNAs extracted from BYL at the indicated times after incubation were subjected to Northern blot analysis using DIG-labeled RNA probe specific to the 3' UTR of RNA3. Relative values for the accumulation of RNAs were calculated and are shown between a pattern on a Northern blot and ethidium-bromide-stained rRNA.



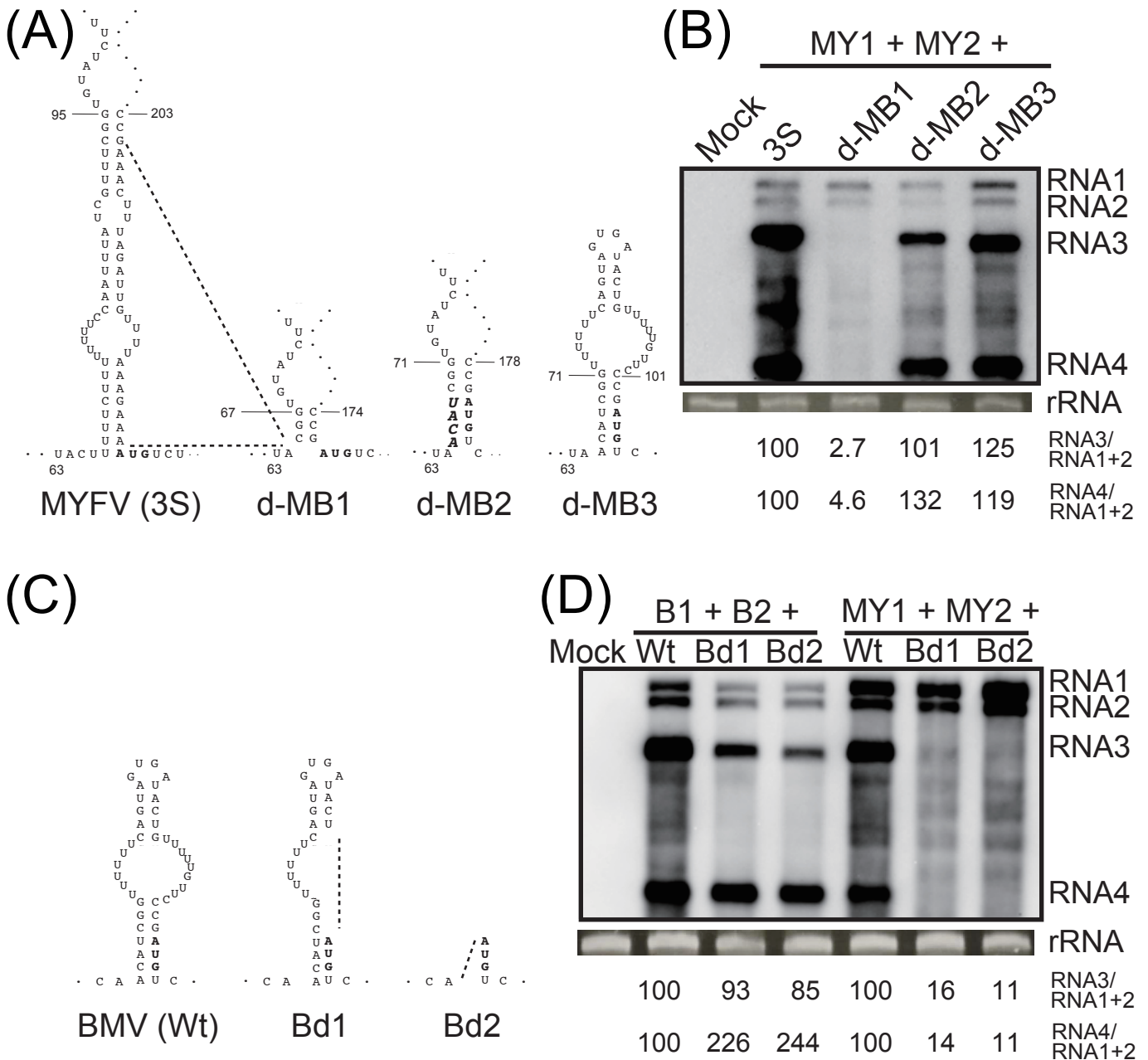


**Fig. II-8. Functional analysis of the similar base-paired structure of BMV RNA3.** (A) Schematic images of the base-paired regions of 3S and its derivatives. Dotted lines and boldface italic letters indicate deleted regions and a four-nucleotide-insertion, respectively. (B) Northern blot analysis of viral RNA accumulation in *N. benthamiana* protoplasts inoculated with 3S or its variants together with MYFV RNA1 and RNA2 (MY1+MY2). A representative result is shown. Numbers below the panel represent the accumulation levels of RNA3 or RNA4 relative to the internal standard (co-inoculated RNA1 and RNA2). The levels were measured using the ImageJ program and the mean values were calculated from three independent experiments. (C) Schematic images of the corresponding structures of BMV RNA3 and its derivatives. Dotted lines indicate deleted regions. (D) Northern blot analysis of viral RNA accumulation in *N. benthamiana* protoplasts inoculated with BMV RNA3 or its variants together with RNA1 and RNA2 of BMV (B1+B2) or the corresponding MYFV RNAs (MY1+MY2). A representative result is shown. The levels were measured using the ImageJ program and the mean values were calculated from three independent experiments.

# Chapter III

## Temporal regulation of viral multiplication via the 5' untranslated region of RNA3 of *Melandrium yellow fleck virus*

### Introduction

In addition to virion formation and genome protection, CPs of plant viruses have multiple roles in virus infection, such as translational regulation, replication, cell-to-cell and long distance movement and suppression of the host defense response (Verchot-Lubicz et al., 2007; Kao et al., 2011; Ni and Kao, 2013). Therefore, in order to achieve successful infection, it is important to regulate the amount and timing of CP expression. Bromovirus CP is translated from RNA4, which is transcribed from negative-stranded RNA3 (Miller et al., 1985; Sacher and Ahlquist, 1989). CP is therefore expressed in the later stage of bromovirus infection. Relatively little is known about the regulatory mechanism(s) of CP expression, despite its importance (Kao et al., 2011).

In this chapter, I analyzed the effects of mutations in the 5' UTR of MYFV RNA3 on the accumulation of viral proteins and found that mutations in a base-paired structure reduced CP accumulation. Time course and polysome profile analyses revealed the temporal regulation of CP translation in MYFV-infected cells.

## Results

### *Deletion mutation in the 5' UTR of RNA3 reduced CP accumulation in Nicotiana benthamiana protoplasts*

The effects of deletion mutations in the 5' UTR of RNA3 of *Melandyrium yellow fleck virus* (MYFV) on the accumulation of 3a protein and CP in *Nicotiana benthamiana* protoplasts were determined. Western blot analysis showed that two deletions (nt 82–103 and nt 203–217) led to a significant reduction in the accumulations of both 3a protein and CP (Fig. III-1B and 1C). This seemed to reflect low levels of RNA3 and RNA4 (Fig. II-2 and III-1C). Deletions of nt 65–81 and nt 218–229 also significantly reduced the accumulation of CP, but the accumulation of 3a protein, RNA3 and RNA4 were not decreased significantly at 20 h post inoculation (hpi) (Fig. III-1B and 1C). This implies that mutations in the 5' UTR of RNA3 affected the accumulation of CP that was translated from subgenomic RNA4. These two sequences (nt 65–81 and nt 218–229) were predicted to form a base-paired structure with each other (Fig. III-1A).

To determine the importance of the base-paired structure for the accumulation of CP, I introduced nucleotide substitutions into both sides of the stem individually and then both sides simultaneously, which respectively disrupted and restored the base-pairing of the stem (Fig. III-2A). The mutation that was introduced into the right side of the stem structure by nucleotide substitutions (3S-c) led to a decrease in CP accumulation. The restoration of the stem (3S-gc) restored the CP levels to that of 3S in *N. benthamiana* protoplasts (Fig. III-2B). The mutation introduced into the left side of the stem structure by nucleotide substitutions (3S-g) had a mild effect on CP

accumulation (Fig. III-2B). This might be caused by an alternative base-pair that is formed with poly-U sequence next to the mutated sequences. These results suggest that the base-paired structure immediately upstream of the 3a-ORF plays a crucial role in CP accumulation in *N. benthamiana* protoplasts.

Next, I constructed mutants of 3S and d218-229 in which the CP gene was replaced with *Renilla* luciferase (R-luc) gene, and the mutant RNA3 molecules were then inoculated into protoplasts together with MYFV RNA molecules 1 and 2. Translational activity was quantitatively evaluated with the dual-luciferase reporter assay system (Promega). Although the levels of accumulated viral RNA molecules were not different at 20 hpi, R-luc activity from d218-229 was greatly reduced, compared to that of 3S (Fig. III-3). This result suggests that these mutations in the 5' UTR of RNA3 are likely to have affected the translation of subgenomic RNA molecules into R-luc or CP, rather than indirectly affecting CP degradation by inhibiting the formation of virions in which assembled CPs were more stable than CPs in non-virion forms, such as monomers. This result also suggests that the reduced CP accumulation was not caused by any function of CP, which has been reported to repress the translation of RNA molecules 1 and 2 in BMV (Yi et al, 2009).

*Deletion mutation in the 5' UTR of RNA3 does not affect translation of RNA4 in trans*

To confirm that direct RNA-RNA interactions were possible between RNA4 and the 5' UTR of RNA3, I searched candidate regions. However, I was not successful at identifying any candidate sequences. Next, to investigate whether interaction between these regions would affect the translation of RNA4 *in trans*, *N. benthamiana* protoplasts were inoculated with RNA3 derivatives and RNA4-CP/R-luc, both in the presence or absence of MYFV RNA molecules 1 and 2. The luciferase activity of firefly Luc was

used as an internal transfection control. In the absence of replication, the translational activity of R-luc was not affected by the 5' UTR of RNA3 (Fig. III-4A). When replication occurred, although the translational activity of R-luc in the presence of RNA3 was 1.5-fold higher than that in the absence of RNA3, no significant difference was observed between 3S and d218-229 (Fig. III-4B). Thus, the 5' UTR of RNA3 does not affect the translation of RNA4 *in trans*, suggesting that the reduction in CP accumulation affected by the 5' UTR of RNA3 was likely to be linked to the synthesis of subgenomic RNA4 from RNA3.

#### *Polysome profile and time course analysis*

To confirm whether the translational activity of RNA4 during viral replication is different between 3S and d218-229, I investigated their translational efficiency in *N. benthamiana* protoplasts using polysome analysis. It is important for polysome analysis to avoid interfering with the distribution of viral RNA molecules by encapsidation in sucrose gradient fractions. Therefore, I confirmed the effect of the F188A mutation in the CP on virion formation, because the corresponding mutation F184A in BMV CP abolishes virion formation (Fig. III-5A; Okinaka et al, 2001). Northern blot analysis of the virion fraction by polyethylene glycol precipitation showed that the F188A mutation in MYFV CP also abolished virion formation (Fig. III-5B). Therefore, I decided to use the F188A mutations for the following assay.

The polysome profile of extracts from MYFV-infected *N. benthamiana* protoplasts treated with cycloheximide at 20 hpi was analyzed by velocity sedimentation in sucrose gradients. As shown in the results for total RNA, the accumulation of viral RNA molecules was indistinguishable between 3S and d218-229 (Fig. III-6A). Unexpectedly, polysome analysis showed that the distribution patterns of RNA4 at 20 hpi were also

indistinguishable between 3S and d218-229 (Fig. III-6B). Moreover, RNA4 was mainly found in light fractions, indicating that the ratio of RNA4 molecules that were bound to ribosomes was low at 20 hpi (Fig. III-6B). These results suggest that the translation of RNA4 may be less efficient at a late stage of viral infection and the polysome analysis should be performed when the translation of RNA4 is active.

To investigate at what point during MYFV multiplication the translation of RNA4 is active, I performed time course analysis of viral replication in *N. benthamiana* protoplasts. In 3S, the levels of accumulated viral RNA molecules and CP almost plateaued at 12 hpi (Fig. III-7). In contrast, the levels of accumulated viral RNA molecules and CP after inoculation with the d218-229 mutant continued to increase, even at 12 hpi. Viral RNAs finally reached to the levels comparable to those observed in 3S. However, at 24 hpi, the levels of accumulated CP in d218-229 were lower compared with those in 3S (Fig. III-7) as shown above (Fig. III-1). Moreover, before 12 hpi, the accumulated viral RNA molecules of d218-229 were lower than those of 3S (Fig. III-7). These results suggest that d218-229 mutation delayed virus multiplication, especially delayed the accumulations of RNA3 and RNA4. However, it is still unclear how this delay causes the low accumulation of CP at a later stage of infection.

From the time course analysis, the level of accumulated CP seemed to plateau at 12 hpi (Fig. III-7), suggesting that CP translation was almost complete by this time point. *N. benthamiana* protoplasts were treated with cycloheximide at 8 hpi to arrest ribosome translation when RNA4 translation was active. As shown in the results from the total RNA analysis, genomic and subgenomic RNA molecules following inoculation with d218-229 accumulated at lower levels than those in 3S (Fig. III-8A). If the translation of RNA4 is inhibited at the stage of initiation, RNA4 would accumulate in the light fractions. However, the pattern of RNA4 distribution in d218-229 in sucrose density

gradients was indistinguishable from that in 3S (Fig. III-8B). Moreover, the ratio of ribosome-bound RNA4 (fractions 6-12) at 8 hpi was higher than that at 20 hpi (Fig. III-9). These results suggest that this mutation did not affect translation initiation of RNA4 at 8 hpi.

Finally, I examined whether the translation of RNA4 was inhibited by the d218-229 mutation after translation initiation at 8 hpi. In this case, ribosome run-off would be slower and polysomes would still be retained in mRNA, despite the absence of cycloheximide (Saini et al., 2009). As shown in Fig. III-10, in the absence of cycloheximide, the distributions of RNA4 shifted to lighter fractions, thereby suggesting that d218-229 mutation-directed repression of translation after initiation did not occur. These results suggest that the reduced accumulation of CP by mutations in the 5' UTR of MYFV RNA3 may be caused by delayed amplification of viral RNA followed by translational repression in the late stage of viral infection as discussed below.

## **Discussion**

In this chapter, I analyzed how mutations in the 5' UTR of MYFV RNA3 affects CP accumulation in *N. benthamiana* protoplasts. First, I identified a novel base-paired structure immediately upstream of the 3a ORF as an RNA element that affected CP accumulation (Fig. III-1). The base substitution that disrupts the base-paired structure as well as deletion mutations in the element reduced CP accumulation (Fig. III-2). The deletion mutation (d218-229) of this structure also reduced the translational activity of R-luc translated from subgenomic RNA4 (Fig. III-3). However, this mutation did not

affect the translational activity *in trans* (Fig. III-4). Polysome analysis by sucrose density gradient showed that the pattern of RNA4 distribution was not different in 3S and d218-229 (Figs. III-6 and 8), suggesting that translational efficiency was comparable between RNA4 of 3S and of d218-229. Time course analysis showed that the mutation resulted in delayed accumulation of MYFV RNA molecules 3 and 4 in *N. benthamiana* protoplasts (Fig. III-7). Moreover, translational repression of RNA4 should occur in the late stage of MYFV infection in *N. benthamiana* protoplasts, which was confirmed by a comparison between the results of polysome analysis at 8 and 20 hpi (Fig. III-9).

The d218-229 mutation delayed MYFV RNAs 3 and 4 accumulation (Fig. III-7). I previously identified an RNA element in the 5' UTR of RNA3 that is required for efficient amplification of negative-strand RNA3 (Chapter II). This RNA element forms a base-paired structure (hereafter referred to as BP1) and is also located near the structure (hereafter referred to as BP2), which was identified in this chapter. I previously showed that a similar base-paired structure located immediately upstream of the 3a ORF in BMV RNA3 could function in the amplification of negative-strand RNA3, and that the structure was conserved among bromoviruses. Therefore, it is possible that BP2 itself has some functions during the amplification of MYFV RNA3. Alternatively, the d218-229 mutation could affect the accumulations of RNA3 and RNA4 due to any effects on the function of BP1. However, since the mutations in BP2 had only a mild effect on RNA3 amplification when compared to those in BP1, levels of viral RNA molecules of d218-229 become indistinguishable from those of 3S in the late stage of viral infection (Fig. III-7).

The results presented here suggest that the synthesis of viral proteins was active in the early stage of MYFV infection, and that it is repressed in the late stage of infection

(Fig. III-9). The d218-229 mutation delays the accumulations of RNA3 and RNA4 (Fig. III-7), and thus the amount of RNA4 that is available as a template for CP synthesis is limited in the early stage of infection when the synthesis of viral proteins is active. The RNA4 of d218-229 continues to be synthesized during infection and finally accumulates to a level similar to that observed in the wild type. However, these RNA4 molecules cannot be used for CP synthesis because protein synthesis is inactive in the late stage of infection (Fig. III-7). Thus, the RNA4 of d218-229 misses the opportunity for CP synthesis, which leads to an imbalance in the levels of accumulated RNA4 and of CP.

Genome packaging of BMV is functionally coupled to replication (Annamalai and Rao, 2006), as reported for other positive-strand RNA viruses (Nugent et al., 1999; Venter et al., 2005). Because this process leads to the specific packaging of viral genomic RNA molecules, it is important to repress synthesis of viral proteins to separate genomic RNA molecules from cellular factors that are involved in translation. In BMV, translational repression was reported for RNA molecules 1 and 2, which is regulated via RNA-protein interactions with the 1a protein (Yi et al., 2007) or with CP (Yi et al., 2009). Although the mechanism of translational repression in bromovirus RNA3 and RNA4 is still unclear, our polysome analysis strongly suggested that translational repression in RNA3 and RNA4 occurs in the late stage of viral infection (Figs. III-6 and 9), thus an as yet uncharacterized mechanism must exist.

Translational repression of eukaryotic cells is induced by several stresses, including heat shock, UV irradiation, hypoxia and viral infection (Anderson and Kedersha, 2002). Phosphorylation of the eukaryotic translation initiation factor (eIF2 $\alpha$ ) is induced by these stresses, which inhibits translation initiation. Subsequently, stress granules are formed, which contain mRNA bound to 48S preinitiation complexes and function as storage sites of cytoplasmic messenger ribonucleoproteins (Anderson and

Kedersha, 2008). Many viruses have been reported to modulate the assembly or disassembly of stress granules to promote virus replication (Valiente-Echeverría et al., 2012). In the late stage of MYFV infection, translation of MYFV RNA molecules was inhibited at the initiation step (Figs. III-6 and -9). It is unclear whether those stress responses in animal and animal virus systems also occur in plants and whether they are induced by MYFV infection. Further study is needed to explain how the translation of RNA3 and RNA4 is repressed.

## **Materials and Methods**

### *Plasmid construction*

pMY3TP4-3Sg, pMY3TP4-3Sc, pMY3TP4-3Sgc: Plasmids with mutations in the 5' UTR of MYFV RNA3 were generated by PCR-mediated site-directed mutagenesis of pMY3TP4-HA (Chapter II): this method is referred to as “recombinant PCR” (Higuchi, 1990). The two pairs of primers used in primary PCR to amplify two DNA fragments were M4 plus stem-g\_R (5'-GAAAAAAAAAGCCCAAGTAAATTCTACAATTAG-3') and stem-g\_F (5'-CTTGGGCTTTTTTTTCCAATTTATCGTTTCG-3') plus MY3.13R-2. The two resultant DNA fragments were recombined by secondary PCR using M4 plus MY3.13R-2. The amplified DNA fragments were purified and digested with *HindIII* and *AccI* and ligated into *HindIII* and *AccI*-cut pMY3TP4-HA to create pMY3TP4-3Sg. pMY3TP4-3Sc was constructed similarly using two pairs of primers, M4 plus stem-c\_R (5'-GACATGGGCTTTAAAACAATCTAAAGTTTC-3') and stem-c\_F (5'-GTTTTAAAGCCCATGTCTAACCTAGTTAAACCC-3') plus MY3.13R-2. pMY3TP4-3Sgc was also similarly constructed using three pairs of primers: M4 plus stem-g\_R, stem-g\_F plus stem-c\_R, and stem-c\_F plus MY3.13R-2.

Replacement of the CP gene with R-luc gene (CP/Rluc): To construct the CP/Rluc series of RNA3, the R-luc gene was amplified by PCR from pSP64-RLUC (Mizumoto et al, 2003) using MYCP/Rluc\_1 (5'-GAACCGTTAAGATGACTTCGAAAGTTTATG-3') plus MYCP/Rluc\_3 (5'-GCAGCAAGGTAGTTATTGTTTCATTTTTGAG-3') primers. Viral elements were amplified from pMY3TP4-HA using MY3.13F (5'-TAATCAAGAGTGCACCG-3') plus MYCP/Rluc\_4 (5'-TCGAAGTCATCTTAACGGTTCAGGTGTTG-3') and MYCP/Rluc\_2 (5'-ACAATAACTACCTTGCTGCCAGTCATAAC-3') plus RV (5'-CAGGAAACAGCTATGAC-3'). The three resultant DNA fragments were recombined by secondary PCR using MY3.13F plus RV. The amplified DNA fragments were purified and digested with *SphI* and *MluI* and ligated into *SphI* and *MluI* -cut pMY3TP4-HA or pMY3TP4-HA-d218-229.

To construct pMY4-CP/Rluc, two DNA fragments were amplified from pMY3TP4-HA using M4 plus sgRNA4\_R (5'-TTTATATATAATATCTATAGTGAGTCGTATTAGCGG-3') and from pMY3TP4-HA-CP/Rluc using sgRNA4\_F (5'-CTAATACGACTCACTATAGATATTATATATAAAATATTTACAC-3') plus RV and were recombined by secondary PCR using M4 plus RV. The amplified DNA fragments were purified and digested with *HindIII* and *EcoRV* and ligated into *HindIII* and *EcoRV* -cut pMY3TP4-HA.

The small *EcoRI* fragment of pBICBPBR2R (Kaido *et al.*, 1997) was treated with T4 DNA polymerase and then inserted into T4 DNA polymerase-treated *KpnI* site of pUBP35 to create pUBP35R. The pUBP35R was cut with *SaII*, blunt-ended with T4 DNA polymerase and ligated with a *BamHI* linker (5'-CGGATCCG-3') to create

pUBP35R-SB. The pUBP35R-SB was cut with *Hind*III, blunt-ended with T4 DNA polymerase and ligated with the *Bam*HI linker to create pUBP35R-SHB. Two DNA fragments were amplified from pUBP35R-SHB using 35R-MS1F (5'-CGCGGATCCTGCAGGCAATTCCCAACATGGTGGAG-3') plus 35R-MS1R (5'-ACGCGTCTAGAATTCCTCGAGAGGCCTCTCCAAATGAAATG-3') and 35R-MS2F (5'-AGGCCTCTCGAGGAATTCTAGACGCGTGATACCCTGTCACCGGATGT-3') plus 35R-MS2R (5'-CGCGGATCCTGCAGGGAGCTTGGCGACGGATCTAT-3') and recombined by secondary PCR using 35R-MS1F plus 35R-MS2R. The amplified DNA fragments were purified and digested with *Bam*HI and ligated into *Bam*HI-cut pUBP35R-SHB, to create pUBP35R-MS.

To construct pUBPMYR4-CP/Rluc, two DNA fragments were amplified from pUBP35R-MS using M4 plus 35S-sg4\_R (TTATATATAATATCCTCTCCAAATGAAATG-3') and pMY3TP4-HA-CP/Rluc using 35S-sg4\_F (TTGGAGAGGATATTATATATAAATATTTAC-3') plus RV and recombined by secondary PCR using M4 plus RV. The amplified DNA fragments were purified and digested with *Sal*I and *Mlu*I and ligated into *Sal*I and *Mlu*I -cut pUBP35R-MS.

To construct pRT-Luc, DNA fragment was amplified from pLucA60 (Mizumoto et al., 2003) using 35S-Fluc\_F (5'-CGGAATTCTAAGGAGATATAACAATGGAAGACGCCAAAAAC-3') plus 35S-Fluc\_R (5'-GGAAAGATCGCCGTGTAAGGTACCCCG-3'). The amplified DNA fragment was purified and digested with *Kpn*I and *Eco*RI and ligated into *Kpn*I and *Eco*RI -cut pRT101 (Töpfer et al., 1987).

CP mutants: To construct the CPF188A series of RNA3, two DNA fragments were amplified from pMY3TP4-HA using MY3.13F plus CPF188A\_R (5'-GTGGGGTGgcATAATCGTCAAGCACAGGCC-3') and CPF188A\_F (5'-CGATTATgcCACCCCCTGCATTAGTTAGC-3') plus RV and recombined by secondary PCR using MY3.13F plus RV. The amplified DNA fragments were purified and digested with *StuI* and *MluI* and ligated into *StuI* and *MluI* -cut pMY3TP4-HA or pMY3TP4-HA-d218-229. To construct pMY3TP4-HA-CPfs, two DNA fragments were amplified from pMY3TP4-HA using MY3.13F plus MYCPfs\_R (5'-GCACGTCTAAGCGGCTGCTCGCCTTTGAG-3') and MYCPfs\_F (5'-GCAGCCGCTTAGACGTGCTGCTAAGCCTC-3') plus RV and recombined by secondary PCR using MY3.13F plus RV. The amplified DNA fragments were purified and digested with *SphI* and *SnaBI* and ligated into *SphI* and *SnaBI* -cut pMY3TP4-HA.

#### *In vitro transcription*

Transcripts of bromoviral RNAs were synthesized using T7 RNA polymerase (Takara, Otsu, Japan) with the cap structure analog (m<sup>7</sup>GpppG; New England Biolabs, Beverly, MA, USA), as described previously (Kroner and Ahlquist, 1992; Chapter I). pLucA60 which had been linearized with *EcoRI* was synthesized using T7 RNA polymerase. All transcripts were purified with Sephadex G-50 (GE Healthcare Bio-Sciences Corp., Piscataway, NJ, USA) gel chromatography.

#### *Dual-luciferase assay*

A total of  $2-3 \times 10^5$  *N. benthamiana* protoplasts transfected with 3.0 µg of transcripts (1 µg each for RNA1, RNA2, and RNA3) were incubated at 25°C for 20 h as described in

Chapter I. Cells were lysed using passive lysis buffer (Promega) and subjected to one or two freeze-thaw cycles to accomplish complete lysis of the cells. Aliquots of cell lysate were assayed with the Dual-Luciferase reporter assay system (Promega), according to the manufacturer's instructions.

To check *trans* activity on translation, under replication non-permissive conditions, protoplasts transfected with 1 µg of RNA3 together with 1µg each of Luc mRNA and RNA4/R-Luc were incubated at 25°C for 6 h and then assayed. Under replication permissive conditions, protoplasts transfected with 3.0 µg of transcripts (1 µg each for RNA1, RNA2, and RNA3) together with 1 µg each of plasmid DNA expressing Luc mRNA (pRT-Luc) and RNA4/R-Luc (pUBPMYR4-CP/Rluc) were incubated at 25°C for 20 h and then assayed. The luciferase activity of R-Luc was normalized to that of firefly Luc, which acted as an internal control. Each experiment was repeated at least three times with different batches of protoplasts.

#### *Encapsidation assay*

For the identification of virion RNAs, viral RNAs were extracted from virion fractions isolated from *N. benthamiana* protoplasts by polyethylene glycol precipitation (Kroner and Ahlquist, 1992) at 20 hpi. These RNAs were detected by northern blot analysis.

#### *Polysome profile*

Protoplasts subjected to polysome analysis were incubated at 25°C for 15 min in the presence or absence of 50 µg/mL cycloheximide. Protoplasts were resuspended in lysis buffer (200 mM Tris-HCl pH 8.0, 200 mM KCl, 25 mM EGTA pH 8.0, 35 mM MgCl<sub>2</sub>, 200 mM sucrose, 5 mM dithiothreitol, 1 mM PMSF, 0.5 mg/mL heparin and 50 µg/mL

cycloheximide) and disrupted with 50 strokes in a Dounce homogenizer. Cell extracts were centrifuged at  $800\times g$  for 10 min at  $4^{\circ}\text{C}$ . Supernatants were mixed with  $0.1\times$  volume of 10% sodium deoxycholate and  $0.05\times$  volume of 20% Triton X-100 and 20% polyoxyethylene sorbitan monolaurate 20 and were then incubated on ice for 15 min. These extracts were centrifuged at  $10,000\times g$  for 5 min at  $4^{\circ}\text{C}$ . Supernatants were layered on 20–50% sucrose gradients prepared in 40 mM Tris-HCl pH 8.0, 200 mM KCl, 10 mM  $\text{MgCl}_2$  and 50 mg/mL cycloheximide, and then centrifuged at  $60,000\times g$  for 14 h at  $4^{\circ}\text{C}$  in a Hitachi RPS40T rotor. Total RNA was purified from each fraction by phenol/chloroform followed by ethanol precipitation.

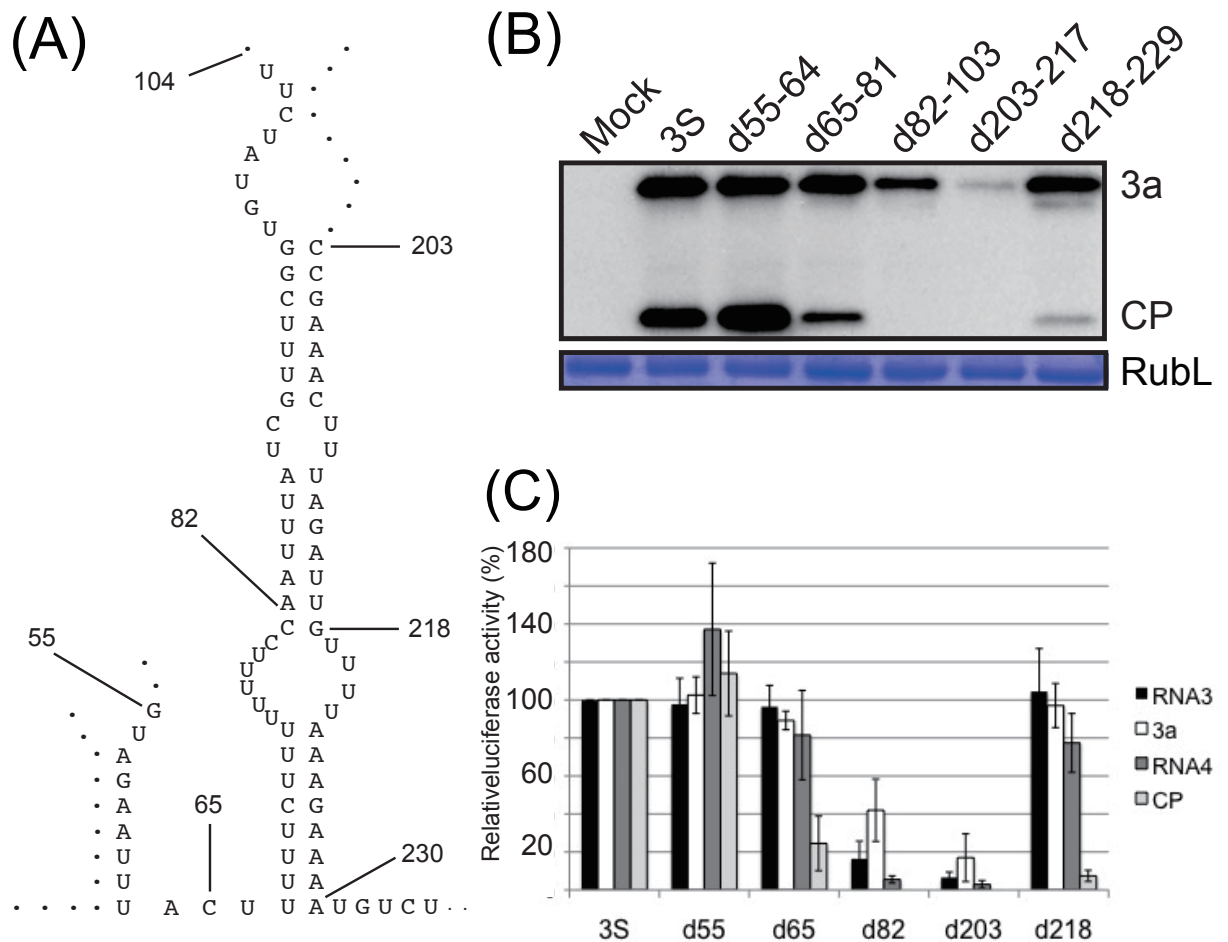


**Fig. III-1. The 5' UTR of MYFV RNA3 affects CP accumulation.** (A) Schematic representation of the predicted secondary structure of the regions, including the *cis*-element for replication of 3S. (B) Western blot analysis of viral protein accumulation in *N. benthamiana* protoplasts inoculated with 3S or its variants together with MYFV RNA1 and RNA2 at 20 hpi. Coomassie brilliant blue stained Rubisco large subunit (RubL) is also shown as a loading control. The representative result is shown. (C) The histogram compares the accumulation levels of RNA3 (black bars), 3a protein (white bars), RNA4 (dark gray bars) and CP (light gray bars) for tested RNA3 derivatives. The accumulation levels were measured using ImageJ program and the mean value and the standard deviation were calculated from at least three independent experiments.

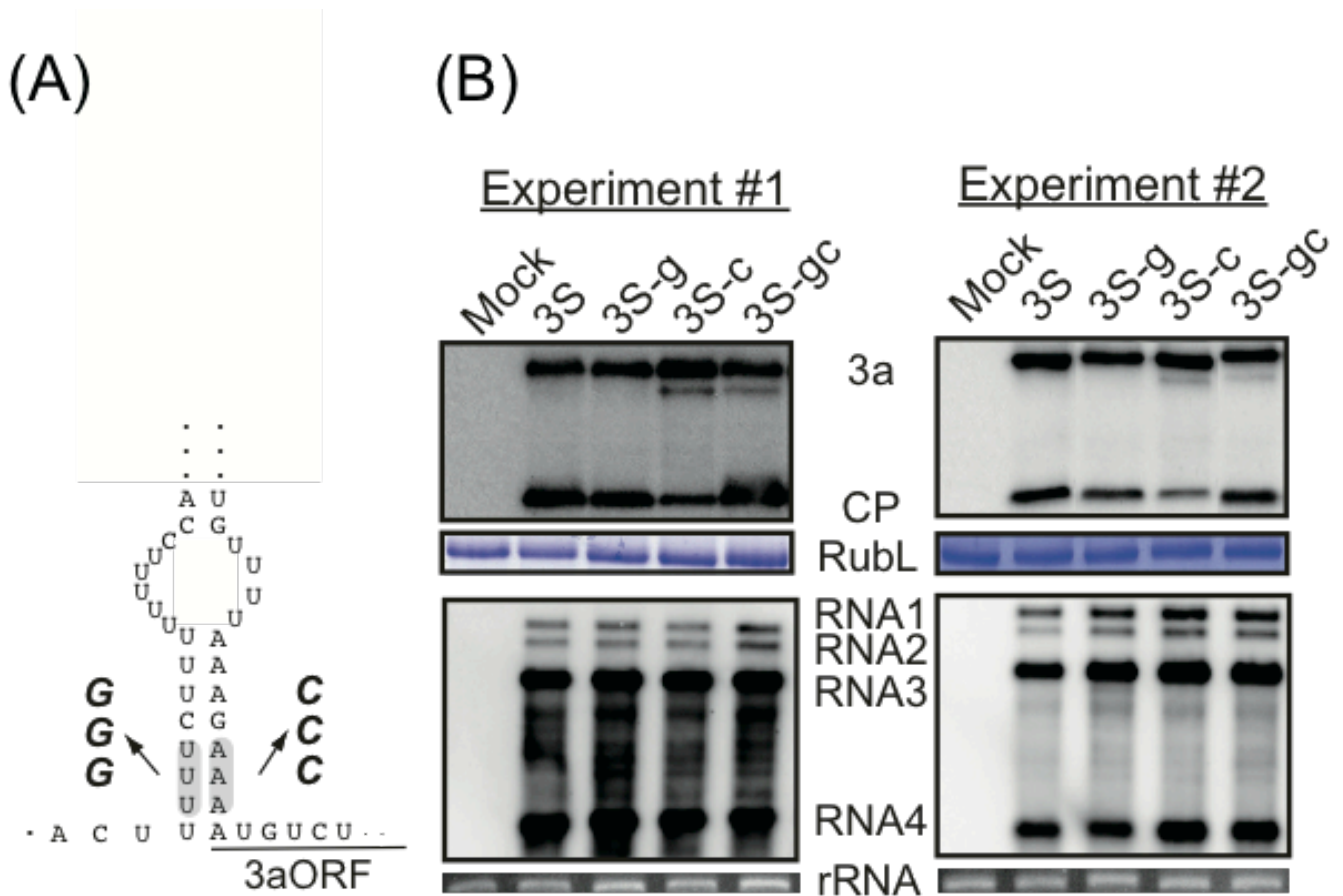


**Fig. III-2. The base-paired structure in the 5' UTR of MYFV RNA3 affects CP accumulation.** (A) Schematic representation of the predicted secondary structure of the regions, including RNA elements affecting the accumulation of CP. Boldface italic fonts indicate substituted nucleotides. (B) Western blot analysis of viral protein accumulation and northern blot analysis of viral RNAs in *N. benthamiana* protoplasts inoculated with 3S or its variants together with MYFV RNA1 and RNA2 at 20 hpi. Coomassie brilliant blue stained Rubisco large subunit (RubL) and ethidium bromide-stained rRNA are also shown as loading controls. The representative result is shown.

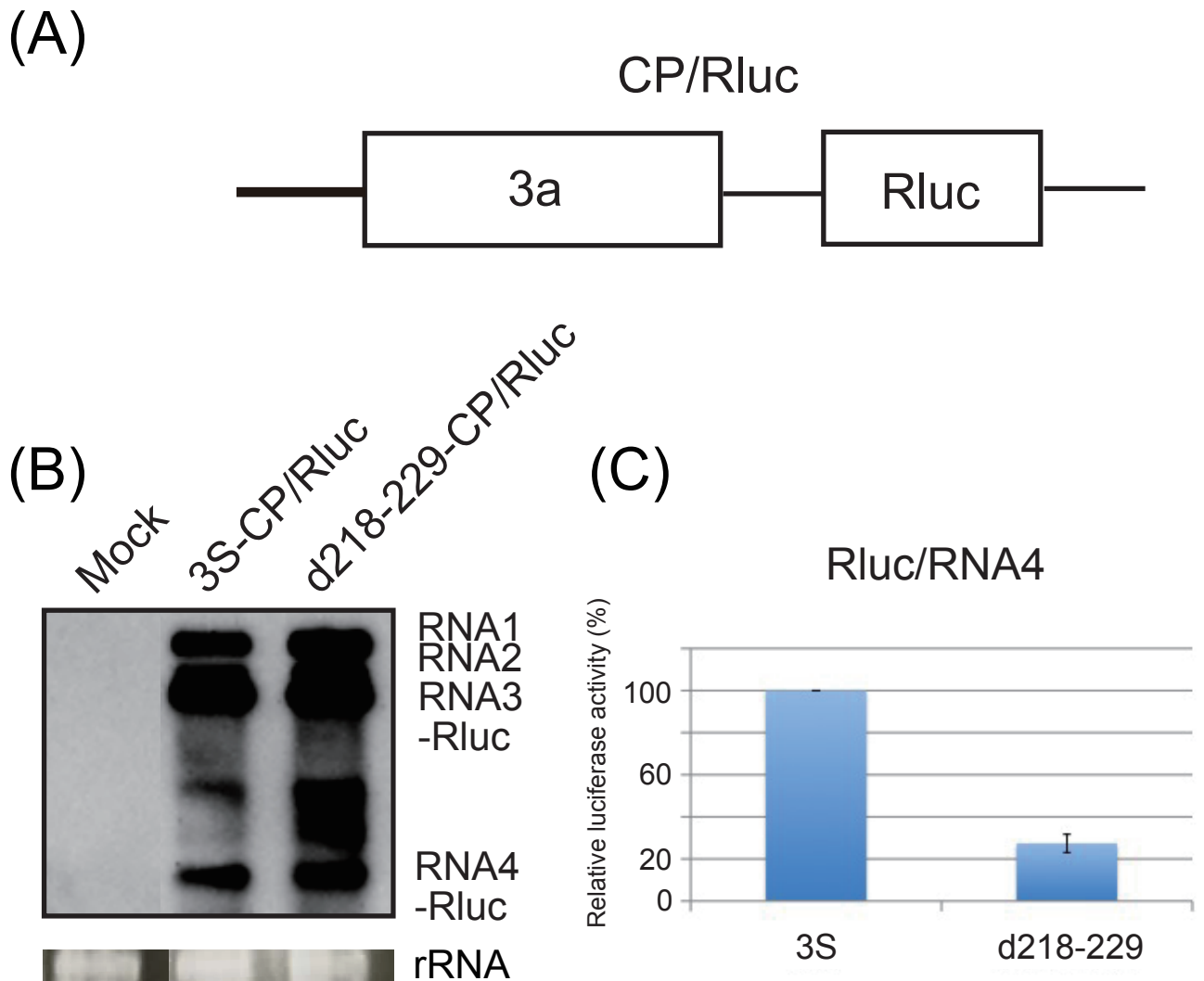
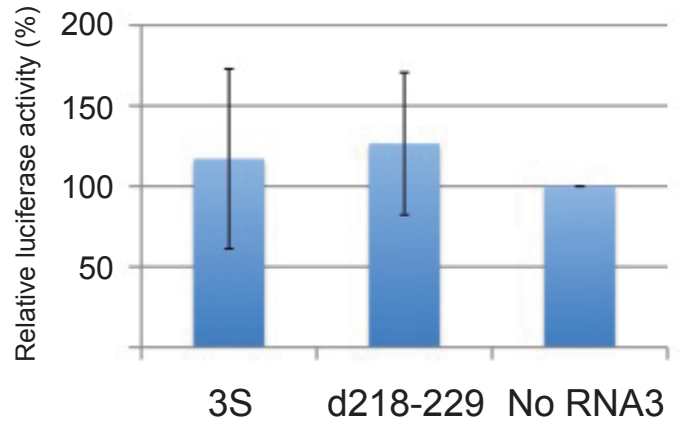
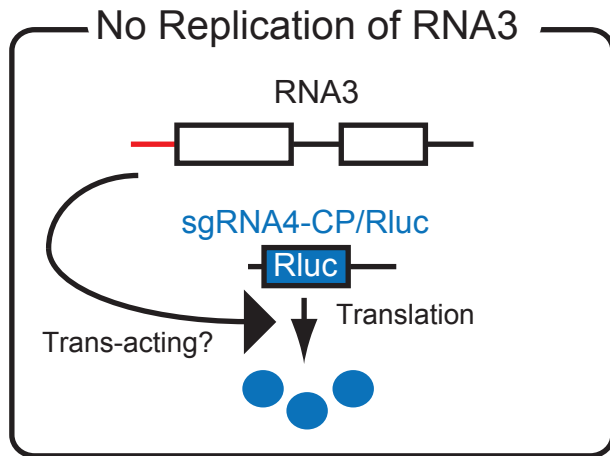


**Fig. III-3. Effect of the deletion mutation of the 5' UTR of MYFV RNA3 on luciferase activity.** (A) The schematic representation of the RNA3 mutants having a *Renilla*-luciferase (Rluc) gene in place of the CP gene. (B) Northern blot analysis of viral RNA accumulation in *N. benthamiana* protoplasts inoculated with the RNA3 mutants having Rluc together with MYFV RNA1 and RNA2 at 20 hpi. The representative result is shown. (C) Relative activities of luciferase compared to the level of its mRNAs, RNA4-Rluc. The mean value and the standard deviation were calculated from five independent experiments.

(A)



(B)

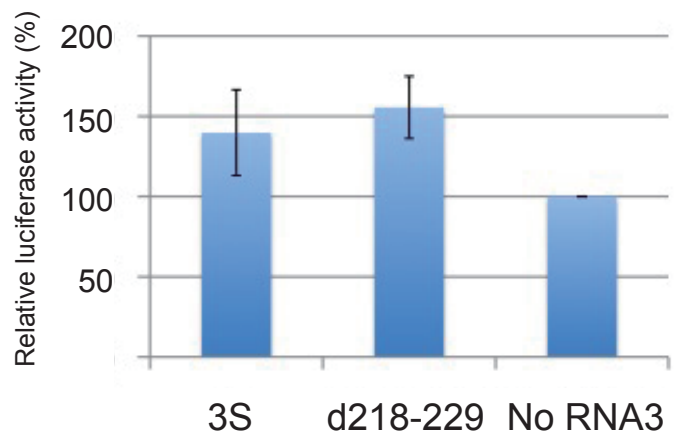
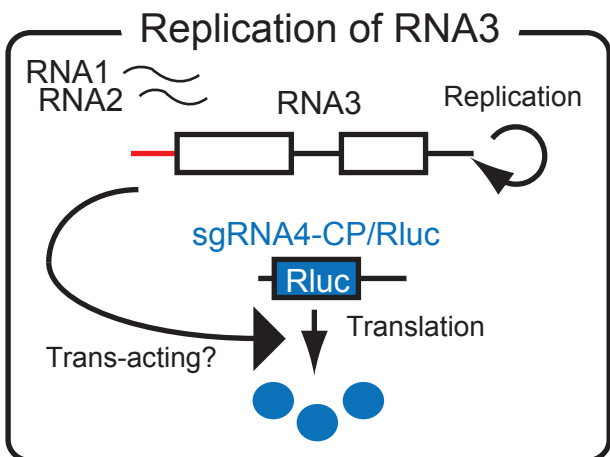


**Fig. III-4. The 5' UTR of MYFV RNA3 does not affect luciferase activities *in trans*.**

(A) Relative activities of luciferase transiently expressed from RNA4 mutants having a *Renilla*-luciferase gene in place of the CP gene, inoculated together with 3S, d218-229 or no RNA3 in *N. benthamiana* protoplasts at 6 hpi. Capped transcripts containing Luc ORF and poly(A)tail (60 nucleotides) were co-transfected as an internal control. The mean value and the standard deviation were calculated from six independent experiments. (B) Relative activities of luciferase transiently expressed from the mutant RNA4 transcribed *in vivo* from plasmid DNA, inoculated together with 3S, d218-229 or no RNA3 in the presence of RNAs 1 and 2 in *N. benthamiana* protoplasts at 20 hpi. The mean value and the standard deviation were calculated from four independent experiments. The plasmid DNA which expresses mRNA containing Luc ORF were co-transfected as an internal control.

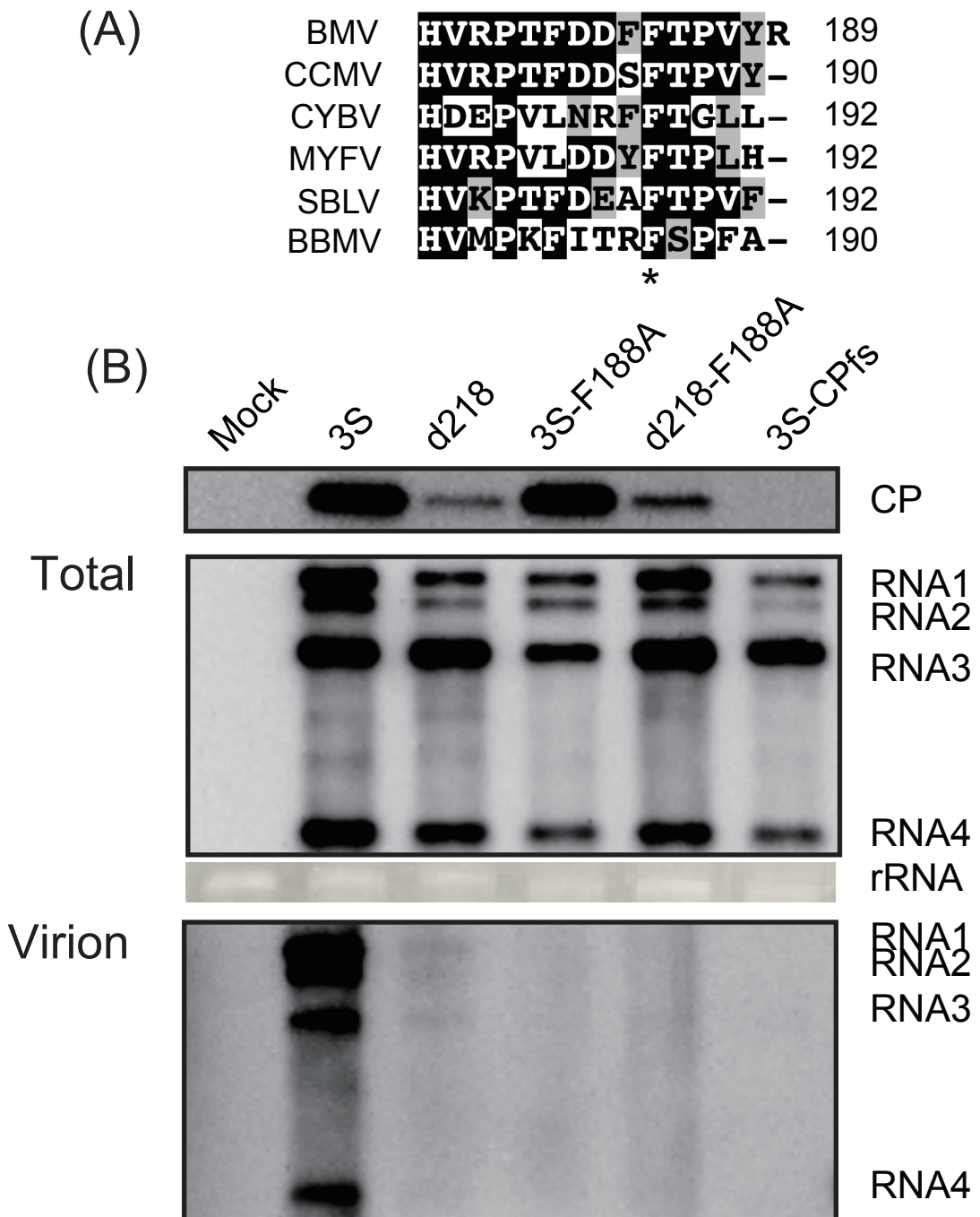


**Fig. III-5. Encapsidation assay.** (A) Alignment of the amino acid sequences of the C-terminal region of the coat protein of bromoviruses. An asterisk denotes the conserved phenylalanine residue whose substitution to alanine abolishes encapsidation in BMV (Okinaka et al., 2001). (B) Western blot analysis of viral protein accumulation in *N. benthamiana* protoplasts inoculated with 3S or its variants together with MYFV RNA1 and RNA2 at 20 hpi. Northern blot analysis of total RNA and the virion RNA fraction extracted from *N. benthamiana* protoplasts. The representative result is shown. In F188A mutants, missense mutation was introduced into the 3'-terminal region of the CP gene of MYFV, which caused an amino acid change from the conserved phenylalanine to alanine at position 188. CPfs represents an RNA3 mutant in which the CP gene has a frameshift mutation.

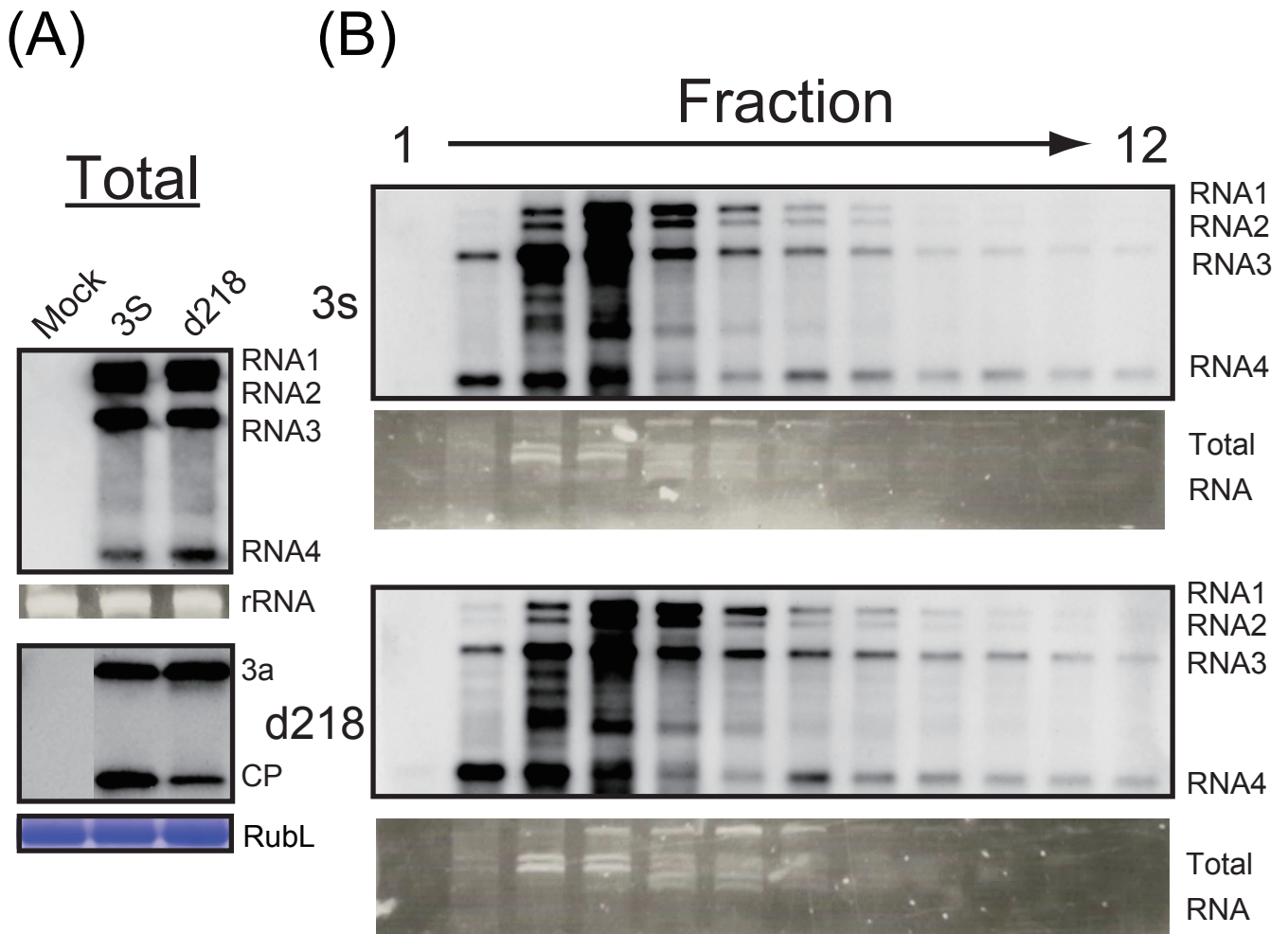


**Fig. III-6. Distribution of viral RNAs in polysome fractions from infected protoplasts at 20 hpi.** (A) Northern blot analysis of viral RNA and western blot analysis of viral protein accumulation in *N. benthamiana* protoplasts at 20 hours after inoculation of F188A mutant of 3S or d218-229 together with MYFV RNA1 and RNA2. (B) *N. benthamiana* protoplasts were treated with 50 µg/ml cycloheximide after 20 hours of incubation and then subjected to sucrose density gradient centrifugation. The distribution of the viral RNAs and total RNA in the gradient fractions was examined by northern blot analysis and ethidium bromide staining, respectively.

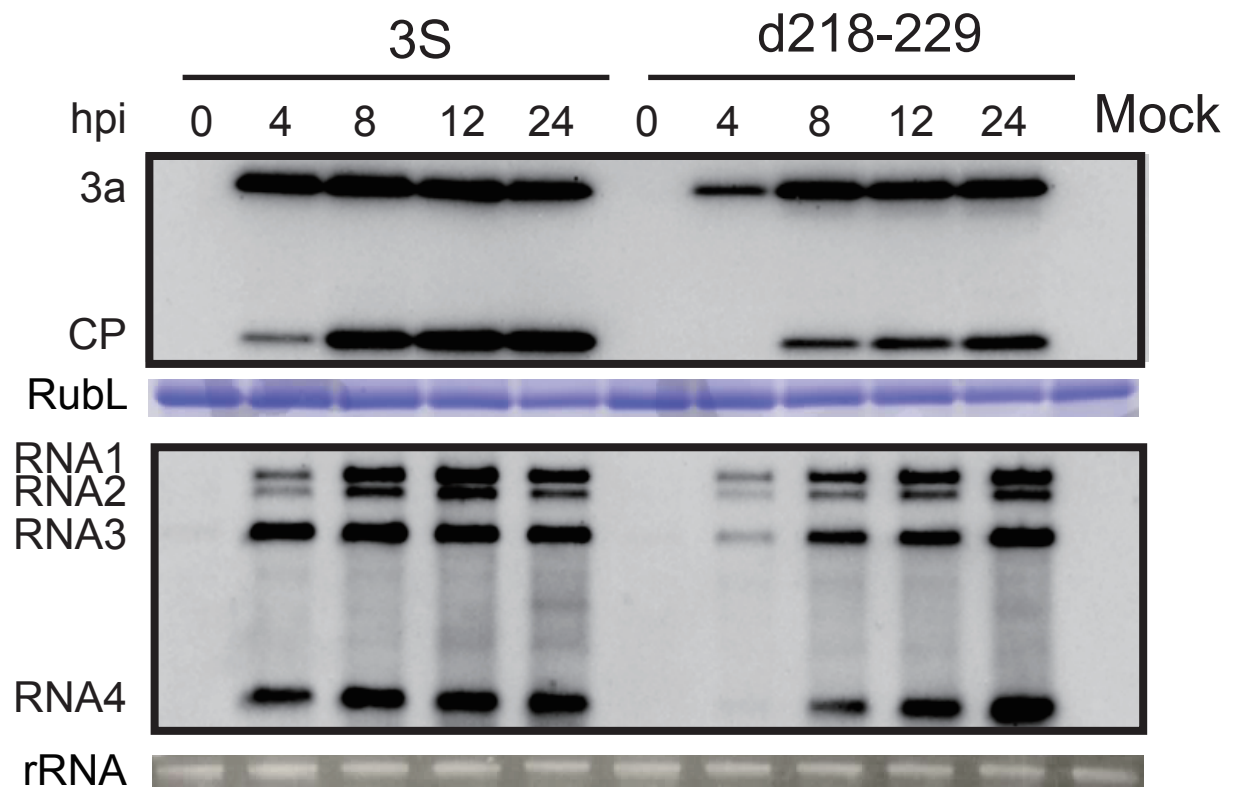


**Fig. III-7. Time course analysis.** *N. benthamiana* protoplasts were inoculated with 3S or d218-229 mutant together with MYFV RNA1 and RNA2. Total proteins and RNAs extracted from protoplasts at the indicated times after inoculation were subjected to western and northern blot analyses, respectively.

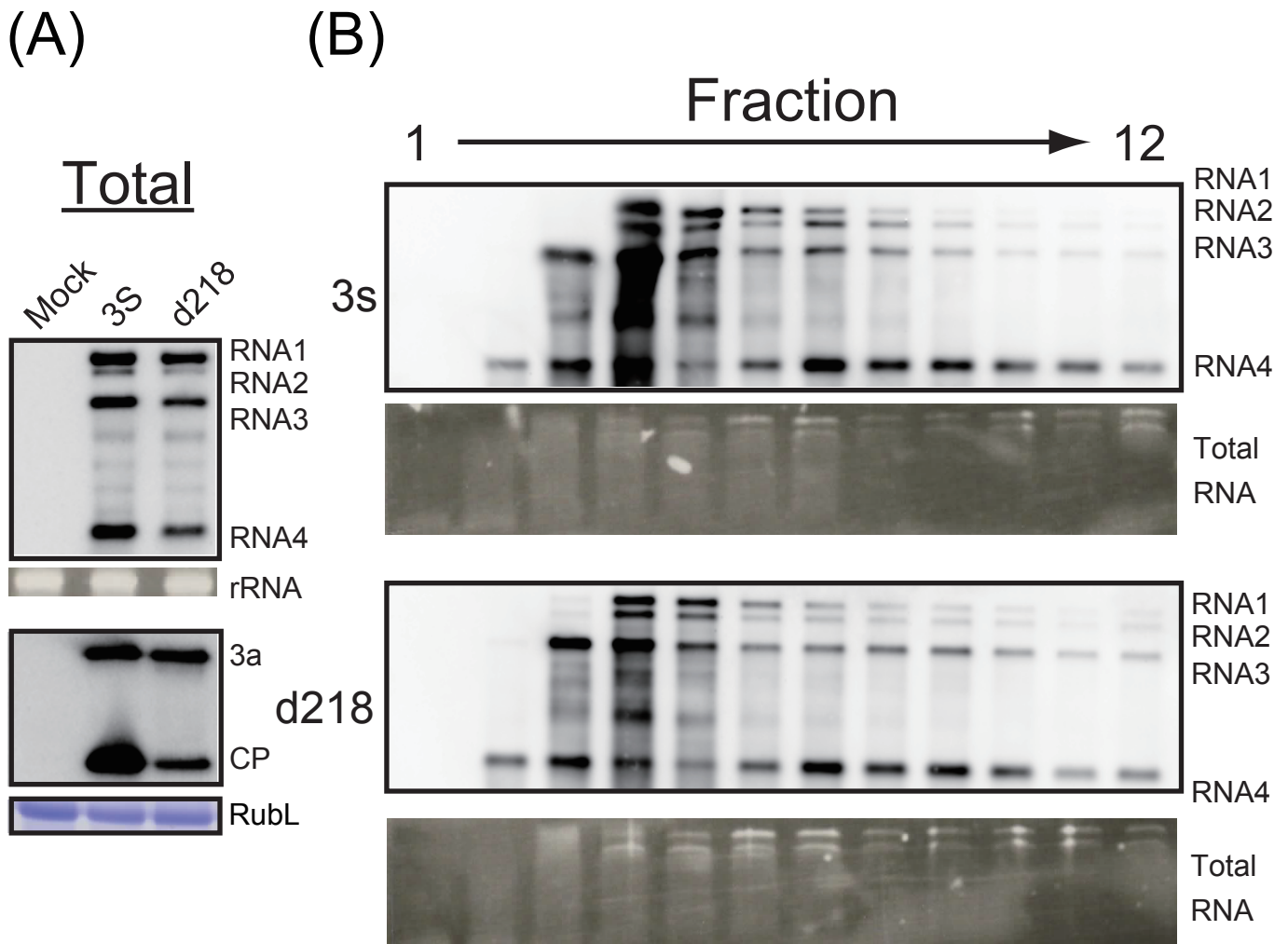


**Fig. III-8. Distribution of viral RNAs in polysome fractions from infected protoplasts at 8 hpi.** (A) Northern blot analysis of viral RNA and western blot analysis of viral protein accumulation in *N. benthamiana* protoplasts at 8 hours after inoculation of F188A mutant of 3S or d218-229 together with MYFV RNA1 and RNA2. (B) *N. benthamiana* protoplasts were treated with 50 µg/ml cycloheximide after 8 hours of incubation and then subjected to sucrose density gradient centrifugation. The distribution of the viral RNAs and total RNA in the gradient fractions was examined by northern blot analysis and ethidium bromide staining, respectively.

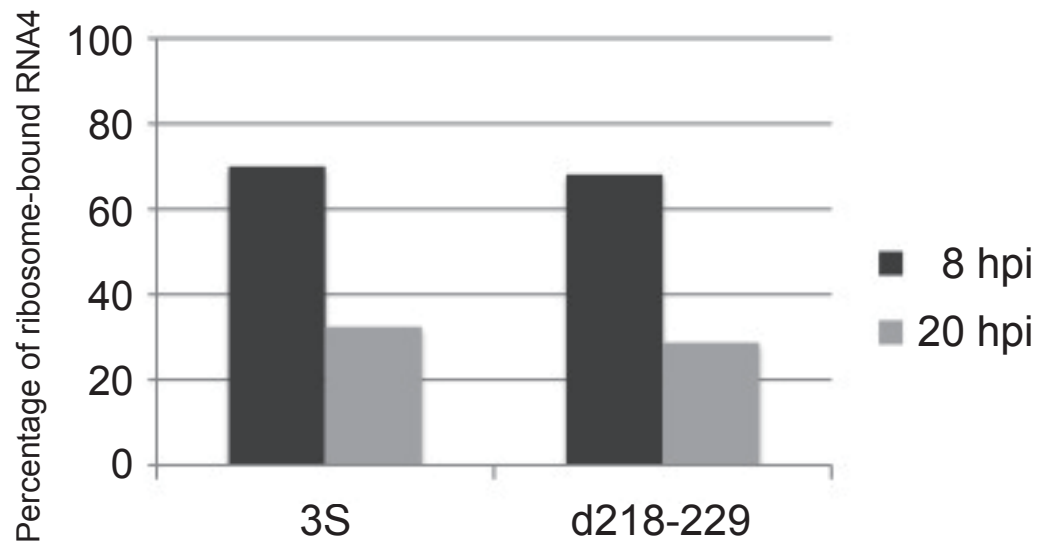


**Fig. III-9. Comparison of polysome profile between the middle and late stages of virus infection.** The ratio of ribosome-bound RNA4 (fractions 6-12) in total RNA4 of 3S and d218-229 at 8 and 20 dpi (Figs. III-6, III-8) were measured using ImageJ program.

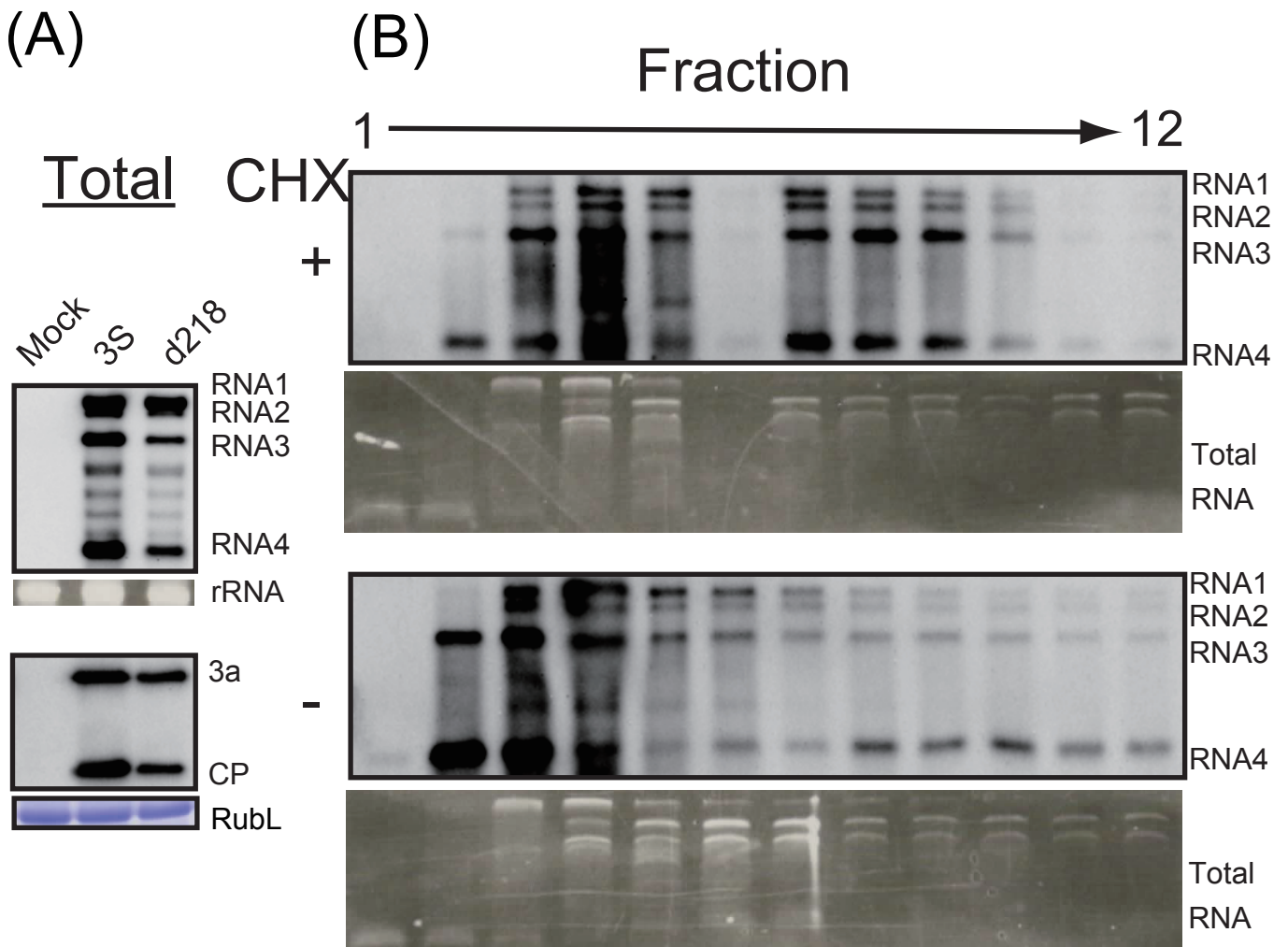


**Fig. III-10. Effects of cycloheximide treatment on the distribution of viral RNAs in polysome at 8 hpi.** (A) Northern blot analysis of viral RNA and western blot analysis of viral protein accumulation in *N. benthamiana* protoplasts at 8 hours after inoculation of F188A mutant of 3S or d218-229 together with MYFV RNA1 and RNA2. (B) *N. benthamiana* protoplasts inoculated with MYFV RNA1, RNA2 and F188A mutant of d218-229 were treated with (+) or without (-) 50 µg/ml cycloheximide after 8 hours of incubation and then subjected to sucrose density gradient centrifugation. The distribution of the viral RNAs and total RNA in the gradient fractions was examined by northern blot analysis and ethidium bromide staining, respectively.

## References

- Agrios GN (2005) Plant pathology 5th ed. *Elsevier Academic Press, San Diego*
- Ahlquist P, Dasgupta R, Kaesberg P (1981a) Near identity of 3' RNA secondary structure in bromoviruses and cucumber mosaic virus. *Cell* 23:183–189
- Ahlquist P, Luckow V, Kaesberg P (1981b) Complete nucleotide sequence of brome mosaic virus RNA3. *J Mol Biol* 153:23–38
- Ahlquist P, Dasgupta R, Kaesberg P (1984a) Nucleotide sequence of the brome mosaic virus genome and its implications for viral replication. *J Mol Biol* 172:369–383
- Ahlquist P, French R, Janda M, Loesch-Fries LS (1984b) Multicomponent RNA plant virus infection derived from cloned viral cDNA. *Proc Natl Acad Sci, USA* 81:7066–7070
- Ahlquist P (2006) Parallels among positive-strand RNA viruses, reverse-transcribing viruses and double-stranded RNA viruses. *Nat Rev Microbiol* 4:371–382
- Ahola T, den Boon JA, Ahlquist P (2000) Helicase and capping enzyme active site mutations in brome mosaic virus protein 1a cause defects in template recruitment, negative-strand RNA synthesis, and viral RNA capping. *J Virol* 74:8803–8811
- Allison RF, Janda M, Ahlquist P (1988) Infectious in vitro transcripts from cowpea chlorotic mottle virus cDNA clones and exchange of individual RNA components with brome mosaic virus. *J Virol* 62:3581–3588
- Allison RF, Janda M, Ahlquist P (1989) Sequence of cowpea chlorotic mottle virus RNAs 2 and 3 and evidence of a recombination event during bromovirus evolution. *Virology* 172:321–330
- Anderson P, Kedersha N (2002) Stressful initiations. *J Cell Sci* 115:3227–3234
- Anderson P, Kedersha N (2008) Stress granules: the Tao of RNA triage. *Trends*

*Biochem Sci* 33:141–150

Annamalai P, Rao AL (2006) Packaging of brome mosaic virus subgenomic RNA is functionally coupled to replication-dependent transcription and translation of coat protein. *J Virol* 80:10096–10108.

Chalfie M, Tu Y, Euskirchen G, Ward WW, Prasher DC (1994) Green fluorescent protein as a marker for gene expression. *Science* 263:802–805

Chapman MR, Kao CC (1999) A minimal RNA promoter for minus-strand RNA synthesis by the brome mosaic virus polymerase complex. *J Mol Biol* 286:709–720

Chen J, Noueiry A, Ahlquist P (2001) Brome mosaic virus protein 1a recruits viral RNA2 to RNA replication through a 5' proximal RNA2 signal. *J Virol* 75:3207–19

Choi SK, Hema M, Gopinath K, Santos J, Kao C (2004) Replicase-binding sites on plus- and minus-strand brome mosaic virus RNAs and their roles in RNA replication in plant cells. *J Virol* 78:13420–13429

Choi YG, Rao AL (2003) Packaging of brome mosaic virus RNA3 is mediated through a bipartite signal. *J Virol* 77:9750–57

Damayanti TA, Nagano H, Mise K, Furusawa I, Okuno T (1999) Brome mosaic virus defective RNAs generated during infection of barley plants. *J Gen Virol* 80:2511–2518

Damayanti TA, Tsukaguchi S, Mise K, Okuno T (2003) *cis*-acting elements required for efficient packaging of brome mosaic virus RNA3 in barley protoplasts. *J Virol* 77:9979–86

Diez J, Ishikawa M, Kaido M, Ahlquist P (2000) Identification and characterization of a host protein required for efficient template selection in viral RNA replication. *Proc Natl Acad Sci, USA* 97:3913–3918

Dreher TW (1999) Functions of the 3'-untranslated regions of positive strand RNA viral

- genomes. *Annu Rev Phytopathol* 37:151–174
- Duggal R, Lahser FC, Hall TC (1994) *cis*-Acting sequences in the replication of plant viruses with plus-sense RNA genomes. *Annu Rev Phytopathol* 32:287–309
- Dzianott AM, Bujarski JJ (1991) The nucleotide sequence and genome organization of the RNA-1 segment in two bromoviruses: broad bean mottle virus and cowpea chlorotic mottle virus. *Virology* 185:553–562
- Filomatori CV, Lodeiro MF, Alvarez DE, Samsa MM, Pietrasanta L, Gamarnik AV (2006) A 5' RNA element promotes dengue virus RNA synthesis on a circular genome. *Genes Dev* 20:2238–2249
- French R, Ahlquist P (1987) Intercistronic as well as terminal sequences are required for efficient amplification of brome mosaic virus RNA3. *J Virol* 61:1457–1465
- French R, Ahlquist P (1988) Characterization and engineering of sequences controlling in vivo synthesis of brome mosaic virus subgenomic RNA. *J Virol* 62:2411–2420
- Frohman MA (1990) RACE: Rapid amplification of cDNA ends In: Innis MA, Gelfand DH, Sninsky JJ, White TJ (eds) PCR protocols. *Academic Press, San Diego*, pp 28–38
- Fujisaki K, Hagihara F, Kaido M, Mise K, Okuno T (2003) Complete nucleotide sequence of *spring beauty latent virus*, a bromovirus infectious to *Arabidopsis thaliana*. *Arch Virol* 148:165–175
- Fujisaki K, Hagihara F, Kaido M, Mise K, Okuno T (2004) Identification and characterization of the *SSB1* locus involved in symptom development by *Spring beauty latent virus* infection in *Arabidopsis thaliana*. *Mol Plant Microbe Interact* 17:967–975
- Fujisaki K, Iwahashi F, Kaido M, Okuno T, Mise K (2009) Genetic analysis of a host determination mechanism of bromoviruses in *Arabidopsis thaliana*. *Virus Res*

140:103–111

- Gamarnik AV, Andino R (1998) Switch from translation to RNA replication in a positive-stranded RNA virus. *Genes Dev* 12:2293–2304
- Grdzlishvili VZ, Garcia-Ruiz H, Watanabe T, Ahlquist P (2005) Mutual interference between genomic RNA replication and subgenomic mRNA transcription in brome mosaic virus. *J Virol* 79:1438–1451
- Gubler U, Hoffman BJ (1983) A simple and very efficient method for generating cDNA libraries. *Gene* 25:263–269
- Hema M, Kao CC (2004) Template sequence near the initiation nucleotide can modulate brome mosaic virus RNA accumulation in plant protoplasts. *J Virol* 78:1169–1180
- Herold J, Andino R (2001) Poliovirus RNA replication requires genome circularization through a protein-protein bridge. *Mol Cell* 7:581–591
- Higuchi, R (1990) Recombinant PCR. In: Innis, M.A., Gelfand, D.H., Sninsky, J.J., and White, T.J. (Eds.), *PCR Protocols. Academic Press, San Diego, CA, USA*
- Hollings M, Horváth J (1981) Melandrium yellow fleck virus. In: CMI/AAB Descriptions of Plant Viruses. *Holywell Press, Oxford*, No 236
- Hull, R (2009) Comparative plant virology. 2<sup>nd</sup> Edition. *Elsevier Academic Press, San Diego, CA, USA*
- Iwahashi F, Fujisaki K, Kaido M, Okuno T, Mise K (2005) Synthesis of infectious in vitro transcripts from *Cassia yellow blotch bromovirus* cDNA clones and a reassortment analysis with other bromoviruses in protoplasts. *Arch Virol* 150:1301–1314
- Iwakawa H-O, Kaido M, Mise K, Okuno T (2007) *cis*-Acting core RNA elements required for negative-strand RNA synthesis and cap-independent translation are

- separated in the 3'-untranslated region of Red clover necrotic mosaic virus RNA1. *Virology* 369:168–181
- Iwamoto T, Mise K, Mori K, Arimoto M, Nakai T, Okuno T (2001) Establishment of an infectious RNA transcription system for Striped jack nervous necrosis virus, the type species of the betanodaviruses. *J Gen Virol* 82:2653–2662
- Janda M, French R, Ahlquist P (1987) High efficiency T7 polymerase synthesis of infectious RNA from cloned brome mosaic virus cDNA and effects of 5' extensions on transcript infectivity. *Virology* 158:259–262
- Janda M, Ahlquist P (1993) RNA-dependent replication, transcription, and persistence of brome mosaic virus RNA replicons in *S. cerevisiae*. *Cell* 72:961–970
- Jayasena KW, Randles JW (2004) A short insert in the leader sequence of RNA 3L, a long variant of Alfalfa mosaic virus RNA3, introduces two unidentified reading frames. *Virus Genes* 29:311–316
- Kaido M, Mori M, Mise K, Okuno T, Furusawa I (1995) Inhibition of *Brome mosaic virus* (BMV) amplification in protoplasts from transgenic tobacco plants expressing replicable BMV RNAs. *J Gen Virol* 76:2827–2833
- Kaido M, Mori M, Mise K, Okuno T, and Furusawa I (1997) Auto-cleavable ribozyme sequence attached to brome mosaic virus cDNAs enhances accumulation of viral RNAs transcribed *in vivo* from the cDNAs. *Ann Phytopathol Soc Jpn* 63, 95–98
- Kao CC, Ni P, Hema P, Huang X, Dragnea B (2011) The coat protein leads the way: an update on basic and applied studies with the brome mosaic virus coat protein. *Mol Plant Pathol* 12:403–412
- Kim CH, Kao CC, Tinoco I Jr (2000) RNA motifs that determine specificity between a viral replicase and its promoter. *Nat Struct Biol* 7:415–423
- Komoda K, Naito S, Ishikawa M (2004) Replication of plant RNA virus genomes in a

- cell-free extract of evacuated plant protoplasts. *Proc Natl Acad Sci, USA* 101:1863–1867
- Kroner P, Richards D, Traynor P, Ahlquist P (1989) Defined mutations in a small region of the brome mosaic virus 2 gene cause diverse temperature-sensitive RNA replication phenotypes. *J Virol* 63:5302–5309
- Kroner PA, Young BM, Ahlquist P (1990) Analysis of the role of brome mosaic virus 1a protein domains in RNA replication, using linker insertion mutagenesis. *J Virol* 64:6110–6120
- Kroner P, Ahlquist P (1992) RNA-based viruses In: Gurr SJ, McPherson MJ, Bowles DJ (eds) *Molecular plant pathology; a practical approach Vol 1*. Oxford University Press, New York, pp 23–34
- Kumar S, Tamura K, Jacobsen I, Nei M (2000) MEGA2: Molecular evolutionary genetics analysis, version 2.0. *Pennsylvania and Arizona State Universities, University Park, Pennsylvania and Tempe, Arizona*
- Laemmli UK (1970) Cleavage of structural proteins during the assembly of the head of bacteriophage T4. *Nature* 227:680–685
- Lane LC (1981) Bromoviruses In: Kurstak E (ed) *Handbook of plant virus infections and comparative diagnosis*. Elsevier/North-Holland Biomedical Press, New York, pp 333–376
- Langereis K, Mugnier MA, Cornelissen BJ, Pinck L, Bol JF (1986) Variable repeats and poly (A)-stretches in the leader sequence of alfalfa mosaic virus RNA 3. *Virology* 154:409–414
- Liu Y, Wimmer E, Paul AV (2009) Cis-acting RNA elements in human and animal plus-strand RNA viruses. *Biochim Biophys Acta* 1789:495–517
- Mas A, Alves-Rodrigues I, Noueir A, Ahlquist P, Diez J (2006) Host

- deadenylation-dependent mRNA decapping factors are required for a key step in brome mosaic virus RNA replication. *J Virol* 80:246–251
- Miller WA, Dreher TW, Hall TC (1985) Synthesis of brome mosaic virus subgenomic RNA in vitro by internal initiation on (-)-sense genomic RNA. *Nature* 313:68–70
- Mine A, Takeda A, Taniguchi T, Taniguchi H, Kaido M, Mise K, Okuno T (2010) Identification and characterization of the 480-kilodalton template-specific RNA dependent RNA polymerase complex of red clover necrotic mosaic virus. *J Virol* 84:6070–6081
- Mise K, Allison RF, Janda M, Ahlquist P (1993) Bromovirus movement protein genes play a crucial role in host specificity. *J Virol* 67:2815–2823
- Mizumoto H, Tatsuta M, Kaido M, Mise K, Okuno T (2003) Cap-independent translational enhancement by the 3' untranslated region of red clover necrotic mosaic virus RNA1. *J Virol* 77:12113–12121
- Narabayashi T, Iwahashi F, Kaido M, Okuno T, Mise K (2009) *Melandrium yellow fleck bromovirus* infects *Arabidopsis thaliana* and has genomic RNA sequence characteristics that are unique among bromoviruses. *Arch Virol* 154:1381–1389
- Narabayashi T, Kaido M, Okuno T, Mise K (2014) Base-paired structure in the 5' untranslated region is required for the efficient amplification of negative-strand RNA3 in the bromovirus m*Melandrium yellow fleck virus*. *Virus Res* 188:162–169
- Navas-Castillo J, Albiach-Martí MR, Gowda S, Hilf ME, Garnsey SM, Dawson WO (1997) Kinetics of accumulation of citrus tristeza virus RNAs. *Virology* 228:92–97
- Ni P, Kao CC (2013) Non-encapsidation activities of the capsid proteins of positive-strand RNA viruses. *Virology* 446:123–132
- Noeiry AO, Ahlquist P (2003) Brome mosaic virus RNA replication: revealing the role of the host in RNA virus replication. *Annu Rev Phytopathol* 41:77–98

- Nugent CI, Johnson KL, Sarnow P, Kirkegaard K (1999) Functional coupling between replication and packaging of poliovirus replicon RNA. *J Virol* 73:427–435
- Ogram SA, Flanagan JB (2011) Non-template functions of viral RNA in picornavirus replication. *Curr Opin Virol* 1:339–346
- Okinaka Y, Mise K, Suzuki E, Okuno T, Furusawa I (2001) The C terminus of brome mosaic virus coat protein controls viral cell-to-cell and long-distance movement. *J Virol* 75:5385–5390
- Pacha RF, Allison RF, Ahlquist P (1990) cis-acting sequences required for in vivo amplification of genomic RNA3 are organized differently in related bromoviruses. *Virology* 174:436–443
- Pacha RF, Ahlquist P (1992) Substantial portions of the 5' and intercistronic noncoding regions of cowpea chlorotic mottle virus RNA3 are dispensable for systemic infection but influence viral competitiveness and infection pathology. *Virology* 187:298–307
- Pathak KB, Pogany J, Nagy PD (2011) Non-template functions of the viral RNA in plant RNA virus replication. *Curr Opin Virol* 1:332–338
- Pogany J, Hung Q, Romero J, Nagy PD, Bujarski JJ (1994) Infectious transcripts from PCR-amplified broad bean mottle bromovirus cDNA clones and variable nature of leader regions in RNA3 segment. *J Gen Virol* 75:693–699
- Pogue GP, Marsh LE, Hall TC (1990) Point mutations in the ICR2 motif of brome mosaic virus RNAs debilitate in the (+)-strand replication. *Virology* 188:742–753
- Pogue GP, Hall TC (1992) The requirement for a 5' stem-structure in brome mosaic virus replication supports a new model for viral positive-strand RNA initiation. *J Virol* 66:674–684
- Quadt R, Ishikawa M, Janda M, Ahlquist P (1995) Formation of brome mosaic virus

- RNA-dependent RNA polymerase in yeast requires coexpression of viral proteins and viral RNA. *Proc Natl Acad Sci, USA* 92:4892–4896
- Romero J, Dzianott AM, Bujarski JJ (1992) The nucleotide sequence and genome organization of the RNA2 and RNA3 segments in broad bean mottle virus. *Virology* 187:671–681
- Roossinck MJ, Bujarski J, Ding SW, Hajimorad R, Hanada K, Scott S, Tousignant M (2005) Family *Bromoviridae* In: Fauquet CM, Mayo MA, Maniloff J, Desselberger U, Ball LA (eds) *Virus taxonomy. Elsevier Academic Press, San Diego*, pp 1049–1058
- Sacher R, Ahlquist P (1989) Effects of deletions in the N-terminal basic arm of brome mosaic virus coat protein on RNA packaging and systemic infection. *J Virol* 63:4545–4552
- Saini P, Eyler DE, Green R, Dever TE (2009) Hypusine-containing protein eIF5A promotes translation elongation. *Nature* 459:118–121
- Saitou N, Nei M (1987) The neighbor-joining method: a new method for reconstructing phylogenetic trees. *Mol Biol Evol* 4: 406–425
- Sarawaneeyaruk S, Iwakawa HO, Mizumoto H, Murakami H, Kaido M, Mise K, Okuno T (2009) Host-dependent roles of the viral 5' untranslated region (UTR) in RNA stabilization and cap-independent translational enhancement mediated by the 3' UTR of Red clover necrotic mosaic virus RNA1. *Virology* 391:107–118
- Sasaki N, Fujita Y, Mise K, Furusawa I (2001) Site-specific single amino acid changes to Lys or Arg in the central region of the movement protein of a hybrid bromovirus are required for adaptation to a nonhost. *Virology* 279:47–57
- Schmitz I, Rao ALN (1996) Molecular study on bromovirus capsid protein; I Characterization of cell-to-cell movement-defective RNA3 variants of brome

- mosaic virus. *Virology* 226:281–293
- Schwartz M, Chen J, Janda M, Sullivan M, den Boon J, Ahlquist P (2002) A positive-strand RNA virus replication complex parallels form and function of retrovirus capsids. *Mol Cell* 9:505–514
- Sivakumaran K, Kim CH, Tayon R, Kao CC (1999) RNA sequence and secondary structural determinants in a minimal viral promoter that directs replicase recognition and initiation of genomic plus-strand RNA synthesis. *J Mol Biol* 294:667–682
- Smirnyagina E, Hsu YH, Chua N, Ahlquist P (1994) Second-site mutations in the brome mosaic virus RNA3 intercistronic region partially suppress a defect in coat protein mRNA transcription. *Virology* 198:427–436
- Sullivan ML, Ahlquist P (1999) A brome mosaic virus intergenic RNA3 replication signal functions with viral replication protein 1a to dramatically stabilize RNA in vivo. *J Virol* 73:2622–2632
- Thompson JD, Higgins DG, Gibson TJ (1994) CLUSTAL W: Improving the sensitivity of progressive multiple sequence alignment through sequence weighting, position-specific gap penalties and weight matrix choice. *Nucleic Acids Res* 22:4673–4680
- Töpfer R, Matzeit V, Gronenborn B, Schell J, Steinbiss JJ (1987) A set of plant expression vectors for transcriptional and translational fusions. *Nucl Acids Res* 15:5890
- Valiente-Echeverría F, Melnychuk L, Mouland AJ (2012) Viral modulation of stress granules. *Virus Res* 169:430-7
- Valverde RA (1985) Spring beauty latent bromovirus: A new member of the bromovirus group. *Phytopathology* 75:395–398

- Venter PA, Krishna NK, Schneemann A (2005) Capsid protein synthesis from replicating RNA directs specific packaging of the genome of a multipartite, positive-strand RNA virus. *J Virol* 79:6239–6248
- Verchot-Lubicz J, Ye CM, Bamunusinghe D (2007) Molecular biology of the potexviruses: Recent advances. *J Gen Virol* 88:1643-1655.;
- Yi G, Gopinath K, Kao CC (2007) Selective repression of translation by the brome mosaic virus 1a RNA replication protein. *J Virol* 81: 1601–1609
- Yi G, Letteney E, Kim CH, Kao CC (2009). Brome mosaic virus capsid protein regulates accumulation of viral replication proteins by binding to the replicase assembly RNA element. *RNA* 15:615–626.
- Zuker M (2003) Mfold web server for nucleic acid folding and hybridization prediction. *Nucleic Acids Res* 31: 3406–3415

## Summary

The infectivity of plant viruses depends on the interactions between host and viral components for the replication of the viral genome, the expression of viral proteins, and the movement of the virus throughout the plant. Bromoviruses are well-studied, tripartite plus-sense RNA plant viruses and six bromovirus species have been reported so far. In this study, I used a bromovirus, *Melandrium yellow fleck virus* (MYFV) with unique characteristics, to analyze the roles of viral components, especially the 5' untranslated region (5' UTR) of genomic RNA3 in viral replication in plants.

### Chapter I

MYFV systemically infected *Arabidopsis thaliana*, although the susceptibility of several *A. thaliana* accessions to MYFV differed from their susceptibility to the other two bromoviruses that infect *A. thaliana*. I constructed full-length cDNA clones of MYFV genomic RNAs 1, 2, and 3 and determined their complete nucleotide sequences. Similarly to the rather distinctive bromovirus *Broad bean mottle virus*, (1) the 5'-terminal nucleotides of the MYFV genomic RNAs were adenine, and (2) the “D-arm” was absent from the tRNA-like structure in the 3' UTRs of MYFV RNAs. As unique characteristics, MYFV RNA3 lacked the poly(A) tract in the intercistronic region and contained a directly repeated sequence of approximately 200 nucleotides and polypyrimidine tracts of heterogeneous lengths in the 5' UTR. Co-infection experiments using RNA3 clones with or without the duplicated sequence demonstrated that the duplication contributed to the competitive fitness of the virus in *Nicotiana benthamiana*.

### Chapter II

Deletion analyses of the 5' UTR of MYFV RNA3 showed that mutations in the short base-paired region, which are located dozens of bases upstream of the initiation codon of the 3a gene, greatly reduced the accumulation of RNA3. Disruption and restoration of the base-paired structure decreased and restored the accumulation of RNA3, respectively. *In vitro* translation/replication assays demonstrated that the base-paired structure is important for efficient amplification of negative-strand RNA3. A similar base-paired structure in *Brome mosaic bromovirus* (BMV) RNA3 functioned in efficient amplification of BMV RNA3, but only in combination with MYFV replicase, and not with BMV replicase, suggesting that there are specific interactions between base-paired structures and MYFV replicase.

### **Chapter III**

Further deletion analyses of the 5' UTR of MYFV RNA3 also showed that mutations in another short base-paired region, which is located immediately upstream of the initiation codon of the 3a gene, greatly reduced the accumulation of coat protein (CP) translated from subgenomic RNA4. However, exploration of intermolecular interactions between RNA3 and subgenomic RNA4 in protoplast assays was not successful, suggesting that the reduced accumulation of CP is linked to the transcription of RNA4 from RNA3. Time-course analysis showed that the mutation resulted in the delay of MYFV replication in *N. benthamiana* protoplasts. Polysome analysis using a sucrose density gradient showed that, although the mutation did not affect the distribution pattern of RNA4, translational repression of RNA4 occurred in the late stage of MYFV infection in *N. benthamiana* protoplasts. These results suggest that the virus needs to synthesize viral RNAs at an optimal time during infection to ensure that viral proteins are expressed for successful replication in cells.

## Acknowledgements

I would like to express my deepest gratitude to Professor Dr. Tetsuro Okuno for his guidance in the field of molecular plant pathology, for his helpful discussion, and valuable suggestions. I also would like to express my gratitude to Professor Dr. Masayuki Sakuma (Kyoto University) and Associate Professor Dr. Takashi Yoshida (Kyoto University) for reviewing this thesis.

I would like to greatly acknowledge to Dr. Kazuyuki Mise for his technical instructions, helpful discussion, valuable suggestions, and for reviewing this article. I would like to express my appreciation to Dr. Masanori Kaido and Dr. Yoshitaka Takano for their valuable suggestions. I am grateful to Dr. Rodrigo A. Valverde (Louisiana State University) for providing MYFV-infected leaves of *Nicotiana clevelandii*, Dr. Yoshihiko Yonezawa (Naruto University of Education) for providing *Melandrium album* seeds, and Dr. Paul Ahlquist (University of Wisconsin) for providing the cDNA clones of BMV.

I greatly appreciate Dr. Fukumatsu Iwahashi, Dr. Hiro-Okii Iwakawa and Dr. Akira Mine for their valuable suggestions and kindness. I also thank all the previous and present members of the Laboratory of Plant Pathology, Kyoto University, for their cheerful support.

Finally, I would like to express my grateful appreciation for my parents, Mr. Riichiro Narabayashi and Ms. Mitsuyo Hashimoto for their generous support throughout my life.

## List of Publications

Narabayashi T, Iwahashi F, Kaido M, Okuno T, Mise K (2009) *Melandrium yellow fleck bromovirus* infects *Arabidopsis thaliana* and has genomic RNA sequence characteristics that are unique among bromoviruses. *Arch Virol* 154:1381–1389

Narabayashi T, Kaido M, Okuno T, Mise K (2014) Base-paired structure in the 5' untranslated region is required for the efficient amplification of negative-strand RNA3 in the bromovirus melandrium yellow fleck virus. *Virus Res* 188:162–169